

Multiple Pulses of the Mantle Plume: Evidence from Tertiary Icelandic Lavas

**HIROSHI KITAGAWA, KATSURA KOBAYASHI, AKIO MAKISHIMA
AND EIZO NAKAMURA***

THE PHEASANT MEMORIAL LABORATORY FOR GEOCHEMISTRY & COSMOCHEMISTRY, INSTITUTE FOR STUDY
OF THE EARTH'S INTERIOR, OKAYAMA UNIVERSITY, MISASA, 682-0193, JAPAN

RECEIVED MARCH 17, 2007; ACCEPTED MAY 26, 2008
ADVANCE ACCESS PUBLICATION JUNE 18, 2008

We present major and trace element concentrations and Sr–Nd–Hf–Pb isotope data for the c. 13–2 Ma Tertiary lavas from eastern Iceland. Our new geochemical results, together with published geological, geochronological, geochemical and geophysical data, are used to evaluate temporal changes in mantle sources contributing to the Tertiary Icelandic magmatism and the relative roles of these sources in magma productivity. The trace element and radiogenic isotopic compositions clearly distinguish three distinct end-member components in the Tertiary magmatism. Temporal variations in lava geochemistry can be attributed to changes in the relative contributions of these three end-member components to the erupted magmas and correlated with temporal variations in magma productivity. The extrusion of lavas with geochemically and isotopically enriched compositions was particularly pronounced at ~13–12 and 8–7 Ma, coincident in time with higher magma productivity. However, the geochemical characteristics of the lavas are different during these two periods: the 13–12 Ma lavas have more radiogenic $^{176}\text{Hf}/^{177}\text{Hf}$ and less radiogenic $^{206}\text{Pb}/^{204}\text{Pb}$ than those erupted from 8 to 7 Ma. The eruption of relatively depleted lavas, at around 10 Ma and younger than 6.5 Ma, is coincident with lower magma productivity. The correlation between the composition and productivity of the Tertiary lavas from eastern Iceland is probably due to periodic changes in the involvement of the enriched end-member component, followed by a gradation to periods dominated by the signature of the depleted end-member component and lower magma productivity, at an approximate frequency of 5 Myr.

KEY WORDS: mantle plume; magma productivity; mantle source; temporal variation; trace element and isotope geochemistry

INTRODUCTION

Hotspot magmatism is thought to be the surface manifestation of partial melting in a mantle plume (Morgan, 1971). However, we still know little about how mantle plumes evolve, and how their evolution contributes to secular changes in long-lived hotspot magmatism. To understand the evolution of long-lived magmatism caused by mantle plumes it is necessary to determine how the compositions and volume of lavas, the products of such magmatism, vary on time scales of millions to tens of millions of years. The North Atlantic province is an excellent target for such studies because the volcanism related to the Iceland mantle plume began at c. 60 Ma and continues to the present day, and has produced voluminous igneous rocks, predominantly basaltic lavas, widely distributed in this region including subaerial Iceland (e.g. Saunders *et al.*, 1997). Iceland is located at the junction between the Kolbeinsey Ridge to the north and the Reykjanes Ridge to the south, and its high magma production rate has been attributed to the interaction between the Iceland mantle plume and the Mid-Atlantic Ridge (MAR), starting at ~27 Ma (e.g. Óskarsson *et al.*, 1985).

Numerous studies of the petrology and geochemistry of Icelandic basalts have been undertaken during the past three decades in an attempt to solve outstanding problems. One of the central subjects of debate is the origin of geochemical diversity in the postglacial lavas, which is probably due to changes in contributions from several different mantle end-member components (e.g. Zindler *et al.*, 1979; Hemond *et al.*, 1993; Chauvel & Hémond, 2000;

*Corresponding author. Telephone: +81-858-43-3745. Fax: +81-858-43-3745. E-mail: eizonak@misasa.okayama-u.ac.jp

Skovgaard *et al.*, 2000; Stracke *et al.*, 2003b). In particular, recent geochemical studies based on comprehensive and precise isotope measurements have attempted to resolve the spatial distribution of different mantle components within the Iceland mantle plume and local mixing trends between them during processes of melt generation and transport (e.g. Thirlwall *et al.*, 2004; Kokfelt *et al.*, 2006).

Although the geochemical variability of the postglacial lavas implies lateral heterogeneity within the mantle, studies of the older Tertiary lavas show that Icelandic magmatism has also varied compositionally during the last 16 Myr, revealing temporal variations in magma source composition (e.g. O'Nions & Pankhurst, 1973; Schilling *et al.*, 1982; Hanan & Schilling, 1997). Hanan & Schilling (1997) first suggested, on the basis of Pb isotope data, that temporal geochemical variations in the Tertiary lavas could be attributed to secular changes in the contributions of three distinct end-member components to the magmatism. They also found a correlation between the composition and productivity of the Tertiary lavas, leading them to a 'blob'-like plume model for the evolution of this magmatism. Additionally, geophysical and palaeoceanographic observations also indicate that there were temporal fluctuations in magma production rate in and around Iceland during the Neogene (e.g. Vogt, 1971; Wright & Miller, 1996). In particular, recent numerical modeling and palaeoceanographic studies have provided detail regarding temporal fluctuations in magma production rate, allowing us to compare precisely the composition of lavas with magma productivity (Jones *et al.*, 2002; Poore *et al.*, 2006).

In this study, we elaborate on the temporal geochemical variation in the Tertiary Icelandic magmatism based on a comprehensive analytical dataset including major and trace element concentrations and Sr–Nd–Hf–Pb isotope ratios of lavas collected along a palaeomagnetic traverse in eastern Iceland. We also provide important constraints on the geochemical characteristics of the end-member source components and evaluate the role of these components in magma productivity. These evaluations in turn allow us to speculate on models for the evolution of Icelandic magmatism.

GEOLOGICAL SETTING AND SAMPLES

The surface exposure of the Icelandic crust is dominantly composed of basaltic lavas (*c.* 90 vol. %) with subordinate amounts of felsic and intermediate rocks (*c.* 10 vol. %) (e.g. Pálmason & Sæmundsson, 1974). The youngest rocks are exposed in the Neovolcanic Zone, which is enclosed by the Pleistocene and Tertiary formations (e.g. Pálmason & Sæmundsson, 1974). The Tertiary formations are well exposed because they are deeply dissected by glacial erosion. According to previous geological investigations

(Walker, 1959, 1964), the dissected fields formed by the Tertiary volcanic rocks can be subdivided into three main geological features: (1) volcanic centers; (2) lava piles (flood basalt successions); (3) swarms of dikes that intrude or constitute feeders for the above. The lava piles are volumetrically dominant in the Tertiary formations. The volcanic centers (e.g. Thingmuli; Carmichael, 1964), characteristically have suites of igneous rocks ranging in composition from basaltic to intermediate (andesitic) and felsic (dacitic and rhyolitic).

In eastern Iceland, Tertiary lavas ranging in age from 13 to 2 Ma are exposed on the plateau. The stratigraphy of this region is well established, and the succession is estimated to be *c.* 10 km in thickness and composed of *c.* 1000 individual flows (Dagley *et al.*, 1967; Watkins & Walker, 1977). The lava piles generally have westerly dips of 5–10° towards the current rifting axes. Consequently, the oldest sequence is exposed on the east coast (Gerpir) and the younger sequence occurs in the west (south of Nordurdalur). The 114 lavas investigated in this study were sampled from successions along a paleomagnetic traverse (labeled A–V in Fig. 1) (Dagley *et al.*, 1967). We have divided the locations of samples into eight separate areas (I–VIII), which correspond to each of the paleomagnetic sections. The locations of samples along the coast of Lagarfljót lake are grouped into an additional area, described here as the Lagarfljót area. This area would correspond sequentially to area VI (or Dagley's N–O–P profiles) (*c.* 6.5 Ma) (McDougall *et al.*, 1976a). The ages assigned to the samples are derived from the magnetostratigraphy and published K–Ar and $^{40}\text{Ar}/^{39}\text{Ar}$ ages obtained for the lavas of this region (Fig. 1).

In general, the lava samples are fine-grained and virtually aphyric or sparsely phryic (generally <10 vol. %) with assemblages of phenocrysts consisting of plagioclase and subordinate amounts of olivine and clinopyroxene. Some of the lavas (II415 and II602) exhibit porphyritic textures with plagioclase being the main phenocryst phase (26–35 vol. %). The groundmasses generally have intergranular textures, and consist of plagioclase, clinopyroxene, an opaque mineral and glass.

ANALYTICAL METHODS

All analyses were performed at the Pheasant Memorial Laboratory, Institute for Study of the Earth's Interior, Okayama University (Nakamura *et al.*, 2003). Samples were crushed with a jaw crusher to coarse chips of 3–5 mm in diameter, and then chips without weathered crusts were carefully selected. These unweathered chips were rinsed several times with deionized water in an ultrasonic bath until the water was clear after rinsing. Chips were then dried for 10 h in an oven at 100°C. The dried chips were pulverized into powders using an alumina puck mill.

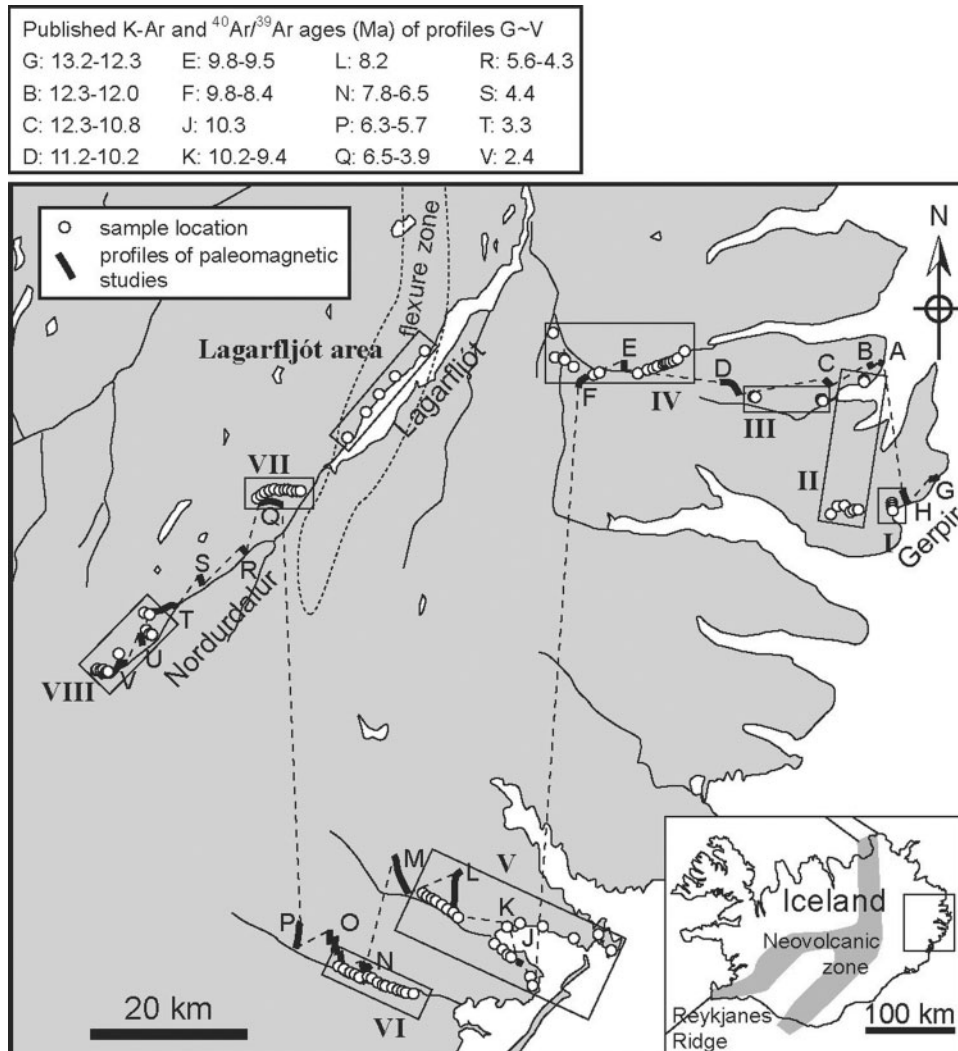


Fig. 1. Map of part of eastern Iceland showing the profiles of the paleomagnetic traverses (Dagley *et al.*, 1967) and the sampling localities (areas labeled I–VIII and Lagarfljót). The ages of each profile are from previous paleomagnetic and geochronological studies (McDougall *et al.*, 1976a, 1976b; Ross & Mussett, 1976; Watkins & Walker, 1977; Mussett *et al.*, 1980).

Concentrations of major elements, Ni and Cr were determined by X-ray fluorescence spectrometry (XRF) with a Philips PW2400 instrument, using lithium tetraborate glass beads (1:10 ratios of sample and flux) (Takei, 2002). Water content (H_2O^+) was obtained by gravimetric methods, and FeO content was determined by titration (Yokoyama & Nakamura, 2002). Trace element compositions were determined by inductively coupled plasma mass spectrometry (ICP-MS) using two systems (Yokogawa PMS2000 and Agilent 7500cs), following the method described by Makishima & Nakamura (1997, 2006), Makishima *et al.* (1997, 1999), Yokoyama *et al.* (1999), Moriguti *et al.* (2004) and Lu *et al.* (2007a). Data are listed in Table 1. Whole-rock analyses, except for the measurements of water content, were duplicated using two aliquots of powdered samples. Analytical errors (1σ) for analyses are

within 1% for major elements and 3–5% for trace elements, respectively (Table 1).

Sr–Nd–Pb isotopic compositions were analyzed by thermal ionization mass spectrometry (TIMS; Finnigan MAT 261 and 262) in static multi-collection mode, following the methods of Yoshikawa & Nakamura (1993) for Sr, and Nakamura *et al.* (2003) for Nd, and the normal double-spike (DS) method for Pb described by Kuritani & Nakamura (2003). Hf isotopes were measured on unspiked samples by multiple-collector (MC)-ICP-MS (Finnigan Neptune) using the method described by Lu *et al.* (2007b). Sr, Nd and Hf isotope ratios were normalized to $^{86}\text{Sr}/^{88}\text{Sr} = 0.1194$, $^{146}\text{Nd}/^{144}\text{Nd} = 0.7219$, and $^{179}\text{Hf}/^{177}\text{Hf} = 0.7325$, respectively, to correct for isotopic fractionation during analysis. Most of the Sr–Nd–Hf isotope measurements were performed on

Table 1: Major and trace element compositions of the Tertiary lavas from eastern Iceland

Sample:	I1501	I1502	I1503	I1504	I1607	I1608	I1605	I1606	I1603	I1604	I1601	I1602	I1505	I1506	I1507
Latitude (°N):	65.032	65.032	65.033	65.033	65.154	65.152	65.155	65.154	65.158	65.158	65.158	65.158	65.024	65.024	65.024
Longitude (°W):	13.596	13.596	13.599	13.607	13.651	13.650	13.652	13.652	13.652	13.651	13.652	13.652	13.694	13.710	13.716
Inferred age (Ma):	12.7	12.7	12.7	12.6	12.8	12.8	12.7	12.7	12.6	12.6	12.5	12.5	12.2	11.9	11.6
Area:	I	I	I	I	II										
<i>Major elements (wt %)</i>															
SiO ₂	47.70	49.59	49.84	47.80	47.22	47.85	47.30	46.13	47.71	46.18	47.46	48.06	47.36	47.25	46.69
TiO ₂	3.28	3.20	2.04	2.54	1.86	3.49	2.55	2.14	3.28	2.04	3.16	1.74	2.68	2.62	2.13
Al ₂ O ₃	13.83	13.24	15.58	14.19	15.83	13.45	14.54	16.42	12.95	15.98	13.24	17.75	13.56	14.06	15.24
Fe ₂ O ₃	7.63	5.93	5.74	6.47	6.49	6.87	6.26	4.58	8.39	3.49	9.21	4.22	6.00	6.64	4.34
FeO	7.28	8.12	5.23	6.93	4.67	8.06	7.21	7.78	6.92	8.09	6.58	5.76	8.01	6.98	7.69
MnO	0.25	0.24	0.19	0.22	0.18	0.24	0.22	0.19	0.26	0.18	0.24	0.16	0.23	0.21	0.19
MgO	4.81	4.11	5.73	5.97	6.38	5.07	6.03	7.28	4.87	6.71	4.75	5.88	5.97	6.05	7.15
CaO	9.80	8.64	10.10	11.05	12.35	9.63	11.31	10.26	9.68	10.42	9.84	11.92	11.09	10.77	11.62
Na ₂ O	2.99	3.27	2.92	2.67	2.28	3.10	2.60	2.49	2.99	2.33	2.89	2.40	2.67	2.77	2.48
K ₂ O	0.50	0.83	0.83	0.49	0.58	0.49	0.43	0.54	0.72	0.46	0.50	0.39	0.50	0.69	0.35
P ₂ O ₅	0.47	0.48	0.33	0.29	0.18	0.46	0.29	0.24	0.40	0.27	0.40	0.20	0.31	0.27	0.21
H ₂ O ⁺	1.83	2.91	1.72	1.59	2.27	1.32	1.63	1.70	2.02	4.14	1.87	1.43	1.41	1.96	2.12
Total	100.37	100.55	100.27	100.21	100.29	100.02	100.36	99.75	100.19	100.30	100.16	99.93	99.78	100.28	100.22
<i>Minor and trace elements (μg/g)</i>															
Cr	41.9	26.5	153	96.7	126	49.9	77.7	93.7	43.9	109	41.2	108	87.9	108	176
Ni	29.4	12.3	79.6	48.9	52.3	26.7	46.8	113	25.4	99.1	25.5	61.4	46.8	49.7	89.0
Li	5.55	4.02	6.67	5.04	8.43	6.14	4.83	5.72	4.42	4.48	4.48	4.47	5.09	5.98	5.38
Be		1.43	1.29		0.655		0.883	0.757		0.858	1.19			0.869	0.694
B	1.37	2.31	1.28	0.726	0.709	1.29	0.600	0.901	0.989	0.541	0.639	0.444	0.863	1.69	1.10
Rb	4.12	10.4	11.4	8.42	13.6	4.27	4.39	11.7	13.5	6.60	7.19	6.11	7.77	10.1	5.95
Sr	327	314	288	308	329	310	324	385	334	356	322	340	322	318	318
Y	51.9	53.1	41.7	35.9	25.0	46.2	33.3	29.5	45.9	32.4	45.2	28.0	37.6	34.4	28.2
Zr	244	276	243	158	106	229	153	136	206	159	208	120	159	152	115
Nb	22.7	26.3	20.6	13.8	9.07	22.1	13.8	11.0	17.7	11.6	17.1	9.25	15.7	13.6	10.2
Cs	0.152	0.162	0.0693	0.0292	0.0586	0.0762	0.0096	0.0252	0.0631	0.0347	0.0738	0.0427	0.0342	0.119	0.288
Ba	186	219	193	119	105	177	129	129	177	111	156	90.2	131	128	85.3
La	24.6	26.2	21.0	14.2	9.44	20.5	13.3	11.1	19.4	13.0	18.6	10.3	14.5	13.2	9.74
Ce	59.9	62.5	48.9	35.8	23.7	50.8	33.8	29.0	48.6	33.4	46.4	26.2	36.3	32.8	24.4
Pr	8.16	8.41	6.57	4.94	3.34	6.74	4.67	4.08	6.55	4.68	6.33	3.66	5.01	4.54	3.40
Nd	37.1	38.4	28.5	23.3	15.8	32.7	22.3	19.3	31.6	21.7	30.1	17.3	24.2	21.6	16.7
Sm	9.01	9.23	6.65	5.91	3.99	7.91	5.61	4.98	7.56	5.44	7.56	4.29	6.01	5.49	4.42
Eu	3.01	3.07	2.13	2.14	1.55	2.72	2.03	1.76	2.76	1.99	2.59	1.61	2.13	2.01	1.63
Gd	9.42	9.52	7.08	6.40	4.26	8.49	6.07	5.36	8.49	5.63	7.98	4.73	6.45	6.06	4.77
Tb	1.54	1.55	1.15	1.07	0.746	1.44	0.991	0.873	1.36	0.925	1.31	0.790	1.07	1.00	0.804
Dy	9.18	9.44	6.80	6.30	4.29	8.00	5.82	5.11	7.97	5.48	7.76	4.80	6.39	6.00	4.73
Ho	1.86	1.87	1.45	1.28	0.892	1.64	1.22	1.07	1.58	1.15	1.61	0.969	1.31	1.21	0.971
Er	4.53	4.79	3.66	3.21	2.28	4.01	3.03	2.69	4.16	2.91	4.04	2.48	3.24	2.99	2.42
Tm	0.662	0.694	0.542	0.470	0.320	0.606	0.444	0.385	0.603	0.413	0.596	0.363	0.485	0.435	0.368
Yb	4.46	4.54	3.57	3.02	2.09	4.04	2.86	2.57	3.83	2.78	3.76	2.40	3.15	2.84	2.28
Lu	0.618	0.633	0.515	0.420	0.288	0.544	0.398	0.350	0.511	0.392	0.541	0.331	0.424	0.397	0.328
Hf	6.22	6.84	5.83	4.06	2.73	5.74	3.83	3.40	5.27	3.89	5.19	3.01	4.14	3.99	3.01
Ta	1.42	1.82	1.40	0.869	0.639	1.44	0.951	0.745	1.09	0.793	1.19	0.642	0.950	0.974	0.707
Pb	2.04	2.06	1.95	1.14	0.722	1.68	1.12	1.01	1.61	1.14	1.60	0.916	1.21	1.04	0.751
Th	2.37	2.58	2.73	1.18	0.780	1.83	1.01	0.817	1.73	0.974	1.51	0.849	1.09	1.08	0.682
U	0.720	0.775	0.780	0.357	0.226	0.543	0.292	0.269	0.551	0.313	0.436	0.264	0.325	0.319	0.220

(continued)

Table 1: Continued

Sample:	I1508	I1509	I1510	IB1608	IB1609	IB1610	IB1606	IB1607	IB1601	IB1602	IB1603	IB1604	IB1605	IB2201	I2201
Latitude (°N):	65.027	65.025	65.019	65.141	65.142	65.142	65.138	65.139	65.130	65.130	65.131	65.131	65.133	65.188	65.180
Longitude (°W):	13.728	13.742	13.765	13.773	13.775	13.775	13.766	13.768	13.945	13.945	13.945	13.946	13.946	14.033	14.063
Inferred age (Ma):	11.3	11.0	10.7	12.4	12.4	12.4	12.3	12.3	11.2	11.2	11.2	11.2	11.2	11.2	11.0
Area:	II	II	II	III	IV	IV									
<i>Major elements (wt %)</i>															
SiO ₂	46.36	49.13	47.44	47.86	44.90	45.00	47.34	46.31	47.11	47.63	48.27	47.71	48.99	48.00	47.46
TiO ₂	2.11	3.41	3.46	2.45	2.11	2.19	2.46	2.37	2.37	3.68	3.35	3.38	3.70	3.79	3.68
Al ₂ O ₃	15.35	12.95	13.83	15.19	16.23	16.16	14.15	14.78	14.99	13.18	13.61	13.29	12.97	12.95	13.32
Fe ₂ O ₃	5.17	6.85	6.53	5.38	5.16	4.55	5.41	6.13	6.80	6.69	6.70	6.61	6.20	7.25	8.03
FeO	6.38	8.06	8.52	6.68	7.46	8.31	7.83	6.35	5.35	8.19	7.79	7.92	8.58	7.85	7.44
MnO	0.17	0.24	0.23	0.19	0.19	0.19	0.21	0.20	0.17	0.26	0.28	0.25	0.25	0.25	0.24
MgO	6.73	4.77	4.75	6.22	7.74	7.55	6.79	6.46	6.10	4.76	4.96	5.07	4.30	4.31	4.61
CaO	11.16	9.17	9.72	11.95	9.80	9.90	11.35	11.21	11.75	9.41	9.77	9.81	8.73	9.16	9.48
Na ₂ O	2.73	2.85	3.01	2.37	2.80	2.68	2.30	2.42	2.36	3.17	3.02	3.06	3.30	3.34	3.01
K ₂ O	0.22	0.47	0.66	0.21	0.53	0.43	0.29	0.51	0.35	0.69	0.61	0.60	0.86	0.79	0.76
P ₂ O ₅	0.25	0.42	0.44	0.29	0.22	0.23	0.23	0.23	0.28	0.51	0.46	0.47	0.73	0.58	0.44
H ₂ O ⁺	3.14	2.10	1.90	1.42	3.40	3.07	1.73	2.54	2.19	1.83	1.66	1.35	1.69	1.37	2.10
Total	99.79	100.42	100.50	100.22	100.55	100.25	100.09	99.51	99.81	100.01	100.47	99.52	100.29	99.65	100.56
<i>Minor and trace elements (µg/g)</i>															
Cr	220	44.7	34.8	163	74.5	77.9	176	281	217	52.0	88.5	82.5	22.7	25.4	43.2
Ni	83.9	26.7	20.2	68.9	109	101	87.6	104	79.8	19.1	37.8	34.8	8.56	8.78	25.3
Li	4.68	5.58	4.11	4.52	6.00	4.54	5.42	7.09	6.14	5.41	5.04	5.60	5.30	5.42	4.25
Be	0.546	1.28	1.24	0.730	0.707	0.697					1.28	1.18	1.10	1.54	1.39
B	1.21	1.52	1.29	0.572	1.92	1.30	0.875	1.08	1.19	1.03	0.862	1.12	1.55	1.48	1.31
Rb	2.14	4.68	9.16	1.34	12.4	7.18	3.22	7.76	4.19	10.8	8.87	9.23	15.8	16.9	14.3
Sr	288	298	350	300	376	364	276	273	320	351	337	336	333	367	333
Y	26.9	50.3	44.0	33.0	26.4	25.6	31.6	32.3	31.9	44.4	42.4	45.2	59.0	55.6	46.7
Zr	118	245	212	142	117	124	129	128	125	215	197	202	281	239	232
Nb	10.2	21.2	21.6	12.7	9.76	10.5	11.6	12.0	11.3	22.9	20.0	20.2	27.9	22.6	24.0
Cs	0.134	0.0545	0.105	0.0034	0.165	0.0567	0.0243	0.213	0.0431	0.0338	0.0677	0.0497	0.0946	0.0983	0.0848
Ba	74.0	163	168	77.7	116	116	80.6	99.2	94.4	173	149	148	218	201	192
La	9.62	21.2	19.9	12.0	9.91	10.7	10.8	11.2	11.6	20.6	18.5	18.9	27.9	24.8	22.7
Ce	24.9	53.7	48.2	30.9	25.0	27.1	27.4	28.7	29.9	50.5	46.3	48.5	68.3	58.5	55.1
Pr	3.49	7.05	6.55	4.31	3.47	3.81	3.83	4.07	4.31	6.88	6.46	6.51	9.36	8.09	7.54
Nd	17.2	33.4	30.6	20.8	16.8	18.0	18.9	19.7	20.4	32.6	29.9	31.0	43.7	37.8	34.0
Sm	4.49	8.40	7.53	5.49	4.32	4.60	5.12	5.20	5.25	8.13	7.49	7.81	10.6	9.06	8.10
Eu	1.67	2.79	2.66	1.98	1.61	1.73	1.88	1.87	1.96	2.98	2.71	2.79	3.64	3.22	2.89
Gd	4.76	8.83	7.99	6.03	4.53	4.84	5.72	5.60	5.87	8.27	7.86	8.35	10.9	9.96	8.56
Tb	0.803	1.48	1.32	1.02	0.757	0.798	0.969	0.930	0.980	1.36	1.28	1.38	1.82	1.56	1.41
Dy	4.76	8.57	7.67	5.97	4.46	4.67	5.73	5.67	5.75	8.04	7.63	7.90	10.4	9.11	8.04
Ho	0.960	1.73	1.54	1.20	0.912	0.944	1.16	1.15	1.12	1.58	1.50	1.62	2.04	1.79	1.67
Er	2.38	4.38	3.84	3.02	2.31	2.41	2.83	2.89	2.84	4.04	3.78	3.95	5.19	4.56	4.18
Tm	0.348	0.632	0.541	0.442	0.338	0.348	0.419	0.424	0.405	0.565	0.531	0.566	0.747	0.634	0.587
Yb	2.30	4.13	3.58	2.80	2.21	2.34	2.73	2.72	2.58	3.65	3.47	3.69	4.96	4.25	3.88
Lu	0.300	0.572	0.495	0.388	0.317	0.318	0.390	0.376	0.362	0.500	0.478	0.509	0.669	0.581	0.515
Hf	2.99	6.17	5.32	3.76	2.95	3.13	3.50	3.52	3.27	5.24	4.94	5.22	6.90	6.10	5.86
Ta	0.715	1.49	1.53	0.895	0.673	0.733	0.742	0.793	0.725	1.58	1.39	1.43	1.92	1.44	1.50
Pb	0.736	1.70	1.48	0.859	0.731	0.870	0.821	0.923	0.886	1.30	1.20	1.33	1.86	1.74	1.71
Th	0.718	2.11	1.63	0.929	0.751	0.739	0.850	0.884	0.866	1.59	1.44	1.55	2.49	1.95	2.00
U	0.186	0.623	0.478	0.272	0.247	0.241	0.253	0.276	0.270	0.521	0.453	0.537	0.775	0.632	0.624

(continued)

Table 1: Continued

Sample:	I2202	I2203	IB2202	I2204	I2205	IB2203	I2206	I2207	I2208	IB2204	I2209	IB2205	I2210	IB2206	I1401
Latitude (°N):	65.178	65.178	65.175	65.174	65.175	65.173	65.170	65.163	65.161	65.156	65.156	65.159	65.159	65.173	64.646
Longitude (°W):	14.081	14.090	14.094	14.097	14.105	14.114	14.124	14.138	14.149	14.167	14.184	14.233	14.257	14.327	14.282
Inferred age (Ma):	11.0	10.9	10.8	10.7	10.6	10.5	10.4	10.3	10.2	10.1	10.0	9.8	9.8	9.6	9.1
Area:	IV	V													
<i>Major elements (wt %)</i>															
SiO ₂	49.86	48.88	46.33	54.60	47.54	48.17	49.39	48.33	48.21	49.82	44.77	47.87	48.81	48.63	45.90
TiO ₂	3.80	3.80	3.66	2.18	2.86	2.92	2.80	3.12	2.55	3.41	3.21	2.60	2.41	2.31	1.85
Al ₂ O ₃	12.54	12.61	13.22	13.27	13.78	14.15	13.70	13.08	14.78	12.86	14.16	13.72	13.60	13.97	16.78
Fe ₂ O ₃	6.40	5.43	9.25	7.38	7.03	3.44	4.69	4.20	3.48	5.23	8.75	5.31	4.50	7.66	4.55
FeO	7.76	9.48	6.24	5.78	7.02	11.04	9.07	10.02	9.00	8.74	7.08	7.73	7.95	5.03	7.10
MnO	0.21	0.23	0.23	0.31	0.24	0.22	0.26	0.23	0.20	0.21	0.29	0.22	0.20	0.22	0.17
MgO	4.55	5.04	5.43	2.62	5.54	5.58	5.40	5.98	5.91	4.83	5.04	6.67	6.83	6.57	8.21
CaO	8.30	9.09	10.12	5.85	10.51	10.64	10.58	10.51	11.48	9.01	7.63	11.44	11.05	11.21	9.87
Na ₂ O	2.65	2.70	2.72	3.98	2.92	2.72	2.56	2.56	2.49	2.84	3.30	2.38	2.38	2.25	2.46
K ₂ O	1.11	0.77	0.36	1.51	0.49	0.39	0.46	0.22	0.26	0.80	0.90	0.18	0.25	0.24	0.31
P ₂ O ₅	0.44	0.43	0.38	1.02	0.38	0.33	0.34	0.30	0.25	0.40	1.38	0.24	0.23	0.20	0.18
H ₂ O ⁺	2.25	1.86	2.26	2.01	1.45	0.38	1.18	1.09	1.64	1.41	3.06	1.09	1.38	2.41	2.75
Total	99.88	100.32	100.18	100.50	99.76	99.98	100.43	99.65	100.24	99.56	99.57	99.45	99.58	100.70	100.14
<i>Minor and trace elements (μg/g)</i>															
Cr	35.6	59.1	71.1	6.03	85.5	60.2	125	110	146	61.1	30.2	91.2	154	212	71.4
Ni	25.9	34.6	42.6	2.66	38.5	45.1	60.0	56.3	62.5	36.3	12.9	72.9	71.9	98.3	149
Li	14.7	7.29	5.92	8.19	7.30	4.91	6.37	5.51	6.38	6.60	6.82	4.56	4.69	4.65	9.25
Be	1.30	1.19	1.09	2.33	1.05	0.890	1.03	1.01	0.808	1.21	2.10			0.701	0.620
B	0.777	0.768	0.680	2.26	0.715	0.921	0.974	0.583	0.701	0.807	1.32	0.736	0.422	0.405	2.02
Rb	27.3	17.9	2.22	32.5	5.26	7.21	8.61	1.41	4.93	15.4	14.1	0.762	2.19	6.00	4.89
Sr	271	294	339	366	330	333	251	264	315	291	372	286	266	226	328
Y	55.8	50.3	44.9	91.5	40.5	41.0	45.0	43.0	33.6	52.2	78.6	35.5	34.9	31.4	23.0
Zr	285	262	211	508	182	150	199	181	141	238	379	136	139	125	103
Nb	23.5	20.7	20.5	44.4	17.0	14.1	16.8	14.5	13.6	23.3	45.7	11.6	10.8	9.66	9.41
Cs	0.457	0.252	0.0081	0.177	0.0163	0.0681	0.0865	0.0089	0.181	0.111	0.0662	0.0037	0.0106	0.0578	0.139
Ba	166	156	132	328	135	116	94.3	80.7	83.9	163	287	67.6	70.0	57.9	74.2
La	22.6	19.7	18.2	46.2	16.3	14.4	14.7	13.2	12.3	21.8	41.5	10.2	10.2	8.64	8.95
Ce	56.5	49.1	45.5	112	41.9	36.5	37.7	35.8	30.4	51.4	103	27.2	27.0	22.9	23.1
Pr	7.80	6.83	6.22	15.1	5.60	4.94	5.46	5.02	4.20	6.85	13.8	3.82	3.86	3.35	3.23
Nd	37.4	33.4	30.1	68.8	26.4	24.9	26.4	24.6	20.1	32.4	64.8	19.4	19.1	16.4	15.5
Sm	9.57	8.86	7.55	16.2	6.69	6.52	6.96	6.58	5.29	8.18	14.9	5.38	5.08	4.52	4.01
Eu	3.06	2.91	2.77	5.69	2.34	2.24	2.29	2.29	1.95	2.76	4.68	1.96	1.86	1.66	1.54
Gd	10.4	9.58	8.09	17.3	7.19	7.06	7.61	7.34	5.94	9.09	15.5	6.08	5.86	5.21	4.20
Tb	1.71	1.53	1.35	2.76	1.19	1.16	1.28	1.23	0.985	1.51	2.39	1.03	0.990	0.885	0.692
Dy	9.63	8.91	7.87	15.6	7.08	7.01	7.79	7.38	5.77	8.82	13.5	6.16	5.88	5.26	4.04
Ho	1.96	1.79	1.58	3.12	1.41	1.38	1.56	1.51	1.20	1.77	2.72	1.24	1.19	1.12	0.819
Er	4.82	4.40	3.84	7.83	3.57	3.50	3.96	3.82	2.95	4.37	6.64	3.11	2.95	2.78	2.00
Tm	0.713	0.648	0.568	1.10	0.523	0.509	0.579	0.559	0.435	0.641	0.958	0.440	0.442	0.404	0.282
Yb	4.50	4.11	3.70	7.08	3.46	3.26	3.83	3.59	2.75	4.12	6.09	2.95	2.87	2.68	1.84
Lu	0.608	0.562	0.496	1.00	0.478	0.457	0.525	0.496	0.392	0.572	0.869	0.412	0.402	0.366	0.256
Hf	7.22	6.59	5.41	11.7	4.62	3.99	5.16	4.78	3.76	6.15	8.60	3.65	3.70	3.36	2.66
Ta	1.69	1.52	1.42	2.90	1.15	0.997	1.20	1.06	0.958	1.68	2.97	0.836	0.789	0.708	0.663
Pb	1.53	1.22	1.20	2.58	1.29	1.06	1.15	1.00	0.868	1.51	1.96	0.805	0.788	0.636	0.622
Th	2.10	1.79	1.49	4.08	1.28	1.15	1.21	1.07	1.00	2.05	2.02	0.782	0.849	0.654	0.706
U	0.709	0.557	0.405	1.33	0.359	0.397	0.406	0.303	0.324	0.668	0.647	0.216	0.295	0.202	0.239

Table 1: *Continued*

Sample:	I1402	IB1401	I1301	I1302	I1303	I1403	I1304	I1404	I1405	I1305	I1406	I1306	I1307	I1308	I1309
Latitude (°N):	64.658	64.649	64.603	64.603	64.610	64.655	64.624	64.654	64.654	64.629	64.653	64.635	64.638	64.663	64.665
Longitude (°W):	14.305	14.345	14.415	14.415	14.420	14.383	14.459	14.432	14.433	14.476	14.456	14.491	14.509	14.568	14.594
Inferred age (Ma):	9.1	9.1	9.0	9.0	9.0	9.0	8.7	8.7	8.7	8.4	8.4	8.3	8.2	8.1	8.1
Area:	V	V	V	V	V	V	V	V	V	V	V	V	V	V	V
<i>Major elements (wt %)</i>															
SiO ₂	48.09	50.56	45.42	45.79	47.63	47.83	45.73	45.52	48.29	47.08	45.85	48.57	47.59	44.95	50.26
TiO ₂	3.23	3.10	2.22	2.17	2.95	3.01	2.23	2.19	2.59	3.59	2.59	2.36	2.47	3.15	2.81
Al ₂ O ₃	13.31	13.12	15.58	15.63	13.76	13.41	14.72	16.16	14.03	13.71	15.29	14.95	15.70	15.74	13.89
Fe ₂ O ₃	7.36	6.69	6.59	5.49	6.23	5.49	5.80	4.86	2.99	6.60	4.13	5.03	5.36	4.89	4.83
FeO	8.26	7.92	6.05	6.93	8.24	9.02	7.19	7.49	9.69	8.53	9.32	7.09	7.23	9.57	8.13
MnO	0.24	0.23	0.17	0.17	0.27	0.24	0.20	0.19	0.20	0.23	0.20	0.18	0.17	0.21	0.21
MgO	4.93	4.70	6.13	8.27	5.49	5.49	8.05	7.92	6.27	5.39	7.42	5.87	5.54	6.13	5.00
CaO	9.48	8.99	10.83	9.47	10.57	10.63	10.32	10.14	11.14	9.60	9.63	11.47	11.08	9.31	9.26
Na ₂ O	3.03	2.89	2.48	2.34	2.75	2.78	2.27	2.28	2.47	2.73	2.85	2.51	2.53	2.73	2.84
K ₂ O	0.53	0.49	0.31	0.34	0.24	0.29	0.36	0.36	0.38	0.47	0.44	0.31	0.37	0.74	0.86
P ₂ O ₅	0.38	0.40	0.21	0.22	0.31	0.33	0.21	0.21	0.25	0.43	0.24	0.24	0.24	0.29	0.36
H ₂ O ⁺	1.08	1.21	3.63	3.12	1.36	1.12	2.58	2.48	1.50	1.92	2.06	1.15	1.45	2.21	1.06
Total	99.93	100.29	99.62	99.94	99.81	99.66	99.66	99.79	99.79	100.27	100.03	99.72	99.75	99.91	99.50
<i>Minor and trace elements (μg/g)</i>															
Cr	42.6	42.5	182	178	78.6	71.4	247	104	166	75.8	90.2	118	79.7	50.0	56.1
Ni	30.5	26.7	183	169	54.1	46.0	145	134	67.0	48.8	121	47.5	65.9	60.8	40.6
Li	9.67	5.42	4.44	21.8	4.18	4.46	5.34	7.27	4.79	4.38	5.11	3.48	4.15	4.75	7.00
Be	1.17		0.609	0.670				0.629			0.736	0.775	0.778	1.00	1.53
B	0.603	1.13	2.63	2.82	0.922	1.22	2.04	1.76	0.922	1.47	0.798	0.548	1.25	1.12	0.978
Rb	4.00	6.15	4.78	6.00	0.925	1.36	6.00	6.27	8.01	6.07	6.48	2.16	5.03	16.5	12.7
Sr	303	268	340	289	323	321	284	305	320	331	302	311	328	636	317
Y	46.6	53.8	28.3	29.1	42.4	43.2	29.6	26.3	38.0	51.2	31.2	32.9	35.1	30.3	51.5
Zr	220	243	115	117	163	177	117	121	151	198	129	148	137	155	249
Nb	19.1	18.0	11.7	11.8	16.9	17.8	13.3	12.9	14.8	20.4	13.1	14.4	13.4	17.0	25.1
Cs	0.0105	0.0606	0.0315	0.130	0.0077	0.0126	0.0644	0.0500	1.59	0.0576	0.0591	0.0104	0.0344	0.0427	0.0688
Ba	159	136	94.5	92.0	117	129	103	96.4	96.2	153	117	107	98.3	169	205
La	17.8	18.9	9.92	10.3	16.2	16.7	11.5	11.1	14.2	20.5	11.4	12.6	12.0	15.6	25.7
Ce	44.6	47.4	25.7	26.5	38.9	40.6	27.9	27.6	34.1	48.7	28.3	31.4	30.1	37.7	61.1
Pr	6.16	6.61	3.64	3.71	5.30	5.63	3.89	3.77	4.69	6.66	3.98	4.37	4.20	5.04	7.85
Nd	29.3	32.4	16.9	17.6	25.4	26.8	18.2	18.1	22.9	31.3	19.1	20.5	20.4	23.3	34.7
Sm	7.48	8.58	4.50	4.55	6.54	6.78	4.66	4.63	6.05	8.07	5.01	5.46	5.39	5.80	8.36
Eu	2.62	2.82	1.65	1.74	2.37	2.46	1.74	1.74	2.21	2.83	1.87	1.94	2.00	2.12	2.64
Gd	7.95	9.26	5.01	5.06	7.25	7.65	5.18	4.93	6.67	8.88	5.44	5.98	5.98	6.01	8.83
Tb	1.35	1.58	0.810	0.819	1.20	1.29	0.881	0.827	1.15	1.46	0.922	1.00	1.01	0.942	1.47
Dy	7.86	9.21	4.92	4.84	7.16	7.59	5.22	4.82	6.76	8.71	5.31	5.87	6.03	5.55	8.68
Ho	1.63	1.91	0.993	1.00	1.44	1.54	1.08	0.982	1.37	1.77	1.09	1.18	1.21	1.09	1.75
Er	4.04	4.78	2.46	2.51	3.62	3.85	2.70	2.53	3.40	4.47	2.84	2.97	2.98	2.60	4.40
Tm	0.596	0.689	0.355	0.369	0.527	0.551	0.395	0.363	0.498	0.639	0.402	0.417	0.431	0.375	0.641
Yb	3.93	4.57	2.30	2.36	3.47	3.61	2.64	2.34	3.22	4.24	2.65	2.71	2.79	2.45	4.25
Lu	0.523	0.624	0.318	0.323	0.475	0.510	0.366	0.327	0.444	0.580	0.371	0.391	0.388	0.334	0.588
Hf	5.46	6.30	3.04	3.03	4.29	4.43	3.10	3.11	3.88	5.09	3.32	3.77	3.56	4.01	6.39
Ta	1.31	1.18	0.799	0.815	1.08	1.21	0.886	0.865	1.01	1.30	0.888	0.966	0.909	1.20	1.79
Pb	1.37	1.55	0.688	0.718	1.01	1.14	0.785	0.759	0.903	1.45	0.779	0.948	0.767	1.07	2.01
Th	1.58	1.73	0.714	0.766	1.43	1.42	0.918	0.900	1.14	1.78	0.900	1.09	0.948	1.26	2.97
U	0.515	0.541	0.239	0.246	0.441	0.430	0.283	0.294	0.356	0.499	0.256	0.343	0.304	0.416	0.890

(continued)

Table 1: Continued

Sample:	I1310	I1311	I1312	I1313	I1314	I1315	I1407	IB1402	I1408	IB1403	I1409	I1410	IB1404	I1411
Latitude ($^{\circ}$ N):	64.681	64.685	64.688	64.692	64.694	64.694	64.606	64.606	64.609	64.614	64.618	64.622	64.623	64.628
Longitude ($^{\circ}$ W):	14.609	14.621	14.639	14.654	14.669	14.686	14.724	14.739	14.751	14.767	14.777	14.799	14.816	14.827
Inferred age (Ma):	8.0	8.0	7.8	7.6	7.5	7.4	8.0	7.8	7.6	7.4	7.2	7.0	7.0	6.9
Area:	V	V	V	V	V	V	VI							

Major elements (wt %)														
SiO ₂	47.93	48.01	48.82	47.90	49.48	50.59	52.36	48.34	49.26	47.84	48.48	48.54	47.71	48.09
TiO ₂	2.69	3.65	3.12	2.65	3.03	3.30	2.76	3.34	2.95	3.82	3.37	2.61	2.06	2.73
Al ₂ O ₃	14.09	13.08	13.14	13.65	13.26	13.01	13.59	13.08	13.71	12.63	13.15	13.94	14.96	14.30
Fe ₂ O ₃	6.83	6.00	4.56	5.28	5.19	5.15	4.32	6.79	5.04	5.87	6.14	5.72	5.78	5.36
FeO	6.41	9.23	10.01	7.98	8.76	9.67	8.38	8.49	9.09	10.10	8.61	7.88	6.00	7.92
MnO	0.19	0.24	0.23	0.20	0.22	0.27	0.27	0.23	0.22	0.24	0.23	0.21	0.21	0.22
MgO	6.62	4.95	5.50	6.37	5.73	4.30	3.52	4.84	5.10	4.83	4.91	5.86	7.16	6.11
CaO	10.67	9.57	10.06	11.25	9.94	8.21	7.18	9.77	9.78	9.41	9.72	10.64	11.72	10.38
Na ₂ O	2.48	2.73	2.81	2.51	2.71	3.16	3.87	2.94	2.82	2.79	2.83	2.68	2.28	2.86
K ₂ O	0.59	0.49	0.43	0.23	0.52	0.71	1.20	0.51	0.40	0.52	0.35	0.34	0.20	0.51
P ₂ O ₅	0.27	0.43	0.35	0.26	0.32	0.51	1.27	0.41	0.33	0.46	0.43	0.28	0.21	0.32
H ₂ O ⁺	1.72	1.95	1.02	1.24	0.68	1.00	1.15	1.69	1.50	1.83	1.51	1.39	1.95	1.19
Total	100.49	100.33	100.05	99.52	99.84	99.87	99.89	100.43	100.18	100.34	99.74	100.08	100.23	99.98
Minor and trace elements (μ g/g)														
Cr	184	43.8	55.8	155	89.1	21.5	8.96	52.2	57.6	44.3	65.3	64.6	175	97.3
Ni	77.6	30.2	42.5	63.2	56.1	10.9	0.01	29.1	41.1	32.7	37.0	45.2	79.1	60.2
Li	5.74	3.77	4.04	3.61	6.29	5.75	4.46	4.30	4.15	3.10	4.44	3.84	3.74	8.90
Be	0.850	1.29	1.11			1.53	1.88	1.15	1.18	0.972	1.19	0.927		0.968
B	0.783	1.11	0.551	0.337	0.769	1.27	1.78	0.817	0.660	0.855	1.01	0.405	0.424	0.913
Rb	8.84	4.61	3.59	1.13	9.87	10.8	25.0	3.93	6.28	5.45	5.26	2.00	0.828	5.24
Sr	295	318	311	261	284	290	420	327	315	317	364	314	292	301
Y	34.8	52.7	46.5	33.6	45.2	57.6	80.5	45.2	46.1	45.9	48.1	37.7	30.4	39.0
Zr	148	230	196	143	195	269	317	207	219	216	229	169	120	171
Nb	14.4	23.6	20.8	13.5	17.5	26.9	33.9	22.2	19.8	22.1	23.1	16.3	11.8	17.0
Cs	0.0105	0.130	0.0532	0.0311	0.0443	0.151	0.148	0.0707	0.139	0.0812	0.432	0.0179		0.0089
Ba	97.3	157	131	76.4	113	165	284	148	148	137	153	111	88.7	120
La	13.1	21.6	17.9	11.3	16.9	25.0	39.0	18.7	18.7	18.0	19.8	14.3	11.0	15.2
Ce	32.5	52.9	44.0	27.9	40.9	60.0	97.0	45.2	45.3	44.3	49.1	35.0	26.8	36.9
Pr	4.60	7.16	5.90	3.97	5.71	8.00	13.2	6.17	6.10	6.17	6.59	4.80	3.62	5.14
Nd	21.5	33.4	28.4	19.2	27.2	37.2	62.0	29.2	28.6	29.9	31.4	22.8	17.5	24.5
Sm	5.56	8.48	7.27	5.05	7.07	9.63	15.2	7.52	7.37	7.82	8.07	5.89	4.61	6.37
Eu	2.05	2.88	2.48	1.81	2.43	3.08	5.19	2.68	2.51	2.87	2.80	2.15	1.74	2.24
Gd	6.05	9.12	7.99	5.76	7.75	10.0	15.83	8.20	7.97	8.47	8.53	6.57	5.16	6.98
Tb	1.03	1.51	1.32	0.957	1.31	1.68	2.51	1.37	1.34	1.40	1.43	1.11	0.869	1.16
Dy	6.05	8.97	7.89	5.80	7.69	9.85	14.0	7.99	8.02	8.14	8.18	6.52	5.06	6.70
Ho	1.22	1.81	1.62	1.17	1.60	2.01	2.79	1.61	1.61	1.64	1.69	1.33	1.01	1.40
Er	3.10	4.51	4.00	2.69	3.95	5.06	6.61	3.93	4.04	3.98	4.26	3.29	2.45	3.39
Tm	0.441	0.666	0.584	0.421	0.577	0.746	0.945	0.570	0.592	0.585	0.599	0.483	0.385	0.498
Yb	2.89	4.27	3.82	2.69	3.78	4.82	6.05	3.68	3.80	3.80	3.89	3.13	2.38	3.16
Lu	0.398	0.586	0.525	0.372	0.540	0.668	0.819	0.510	0.526	0.514	0.535	0.437	0.323	0.430
Hf	3.83	6.03	5.24	3.90	5.03	7.08	8.05	5.37	5.66	5.30	5.71	4.29	3.13	4.32
Ta	1.00	1.69	1.26	0.891	1.08	1.93	2.11	1.55	1.41	1.53	1.60	1.15	0.769	1.19
Pb	0.885	1.46	1.26	0.775	1.23	1.80	2.04	1.21	1.43	1.11	1.36	1.07	0.730	1.38
Th	1.05	1.92	1.61	0.909	1.48	2.30	3.44	1.71	1.86	1.52	1.90	1.35	1.00	1.34
U	0.331	0.583	0.504	0.282	0.475	0.676	1.11	0.529	0.563	0.438	0.550	0.374	0.297	0.384

(continued)

Table 1: Continued

Sample:	IB1405	IB1406	I1412	I1413	I1414	I1415	I1416	I1417	I1418	I2118	I2117	I2116	IB2110	I2115
Latitude ($^{\circ}$ N):	64.621	64.621	64.624	64.625	64.626	64.628	64.630	64.633	64.641	65.177	65.135	65.118	65.094	65.076
Longitude ($^{\circ}$ W):	14.837	14.840	14.851	14.861	14.875	14.891	14.908	14.918	14.928	14.650	14.749	14.781	14.821	14.863
Inferred age (Ma):	6.8	6.8	6.8	6.7	6.7	6.6	6.6	6.5	6.5	6.7	6.6	6.5	6.5	6.5
Area:	VI	Lagarfljót	Lagarfljót	Lagarfljót	Lagarfljót	Lagarfljót								
<i>Major elements (wt %)</i>														
SiO ₂	48.88	48.01	50.12	49.48	52.15	46.44	52.36	48.30	47.74	48.76	47.80	48.73	48.40	48.93
TiO ₂	3.84	2.22	3.52	3.37	3.07	1.31	1.91	3.03	1.95	2.93	2.36	2.63	2.48	2.99
Al ₂ O ₃	13.35	14.69	13.33	12.88	13.56	18.58	15.18	12.99	15.71	13.40	14.09	13.61	14.79	13.08
Fe ₂ O ₃	5.89	5.33	5.59	6.44	5.68	5.74	5.59	6.42	6.36	3.01	5.63	4.69	5.27	4.99
FeO	8.58	6.57	8.57	8.36	7.50	3.51	6.38	8.77	4.84	10.76	7.08	8.91	7.31	9.09
MnO	0.25	0.20	0.24	0.25	0.24	0.14	0.30	0.24	0.18	0.22	0.20	0.22	0.21	0.23
MgO	4.59	6.62	4.45	5.02	4.45	5.93	2.69	5.12	6.30	5.89	6.33	5.96	5.94	5.48
CaO	8.89	11.34	8.43	9.23	8.06	12.70	6.39	9.63	11.60	10.54	11.68	10.61	11.08	9.92
Na ₂ O	3.08	2.44	3.25	2.71	3.10	2.04	4.24	2.81	2.69	2.66	2.26	2.68	2.65	2.66
K ₂ O	0.85	0.28	1.03	0.34	1.01	0.17	1.61	0.45	0.30	0.50	0.19	0.40	0.43	0.38
P ₂ O ₅	0.62	0.30	0.47	0.36	0.67	0.14	1.21	0.40	0.20	0.34	0.23	0.29	0.26	0.32
H ₂ O ⁺	1.35	1.67	0.55	1.71	0.93	3.30	1.84	1.45	2.32	0.90	2.27	1.00	1.16	1.52
Total	100.17	99.66	99.55	100.15	100.44	99.99	99.72	99.61	100.18	99.91	100.12	99.73	99.98	99.60
<i>Minor and trace elements (μg/g)</i>														
Cr	33.8	193	26.2	54.2	38.3	227	3.51	53.3	214	109	187	103	146	59.1
Ni	15.5	78.2	15.7	39.4	13.2	84.5	0.01	31.4	69.8	55.9	69.9	51.2	55.1	40.2
Li	8.41	3.34	4.92	8.56	11.9	4.07	8.39	5.24	4.92	3.41	5.20	5.18	4.34	5.43
Be	1.39		1.45	1.01	1.45	0.440	2.75		0.637	1.03	0.728	0.946		1.09
B	1.39	0.680	1.07	0.527	0.594	1.08	3.20	0.938	0.639	1.08	0.581	0.778	0.563	0.594
Rb	15.2	1.87	23.8	2.54	15.6	1.62	31.4	4.60	2.07	9.40	1.06	4.57	4.68	4.87
Sr	310	299	298	277	322	325	408	289	265	293	268	260	292	286
Y	55.8	33.2	53.1	47.9	55.4	19.5	89.1	51.7	28.6	43.1	29.8	41.0	36.4	43.9
Zr	267	150	275	214	265	73.6	547	207	115	194	123	167	150	205
Nb	25.2	13.3	26.3	18.9	23.1	6.05	52.4	18.6	9.23	16.7	12.0	14.2	12.5	16.4
Cs	0.0431	0.0323	0.132	0.0158	0.0350	0.190	0.215	0.0935	0.0457	0.163	0.0084	0.0244	0.0091	0.0485
Ba	175	95.2	182	108	197	53.3	378	121	77.3	102	67.1	96.4	98.2	113
La	24.1	13.2	23.8	17.8	25.3	6.02	54.0	18.2	9.12	15.4	10.6	12.8	12.5	16.2
Ce	59.0	33.2	59.3	43.7	61.9	15.8	130	45.2	22.9	40.1	26.7	32.7	31.2	40.6
Pr	8.09	4.66	7.85	6.09	8.37	2.18	17.2	6.27	3.27	5.41	3.78	4.60	4.29	5.59
Nd	38.5	21.7	36.0	29.3	39.2	10.6	78.0	30.5	15.9	26.0	18.1	22.5	21.0	26.7
Sm	9.47	5.28	8.72	7.54	9.53	2.89	17.5	7.84	4.27	6.81	4.76	6.02	5.61	6.88
Eu	3.33	1.90	2.98	2.65	3.38	1.13	5.55	2.68	1.58	2.35	1.76	2.12	1.99	2.39
Gd	10.1	5.93	9.32	8.11	10.2	3.23	17.7	8.78	4.84	7.45	5.10	6.73	6.31	7.63
Tb	1.63	0.969	1.53	1.39	1.65	0.547	2.74	1.47	0.824	1.26	0.867	1.15	1.05	1.27
Dy	9.63	5.84	8.97	8.21	9.46	3.40	15.6	8.72	4.97	7.49	5.15	6.92	6.23	7.49
Ho	1.93	1.19	1.81	1.68	1.89	0.702	3.10	1.78	1.02	1.51	1.07	1.44	1.26	1.51
Er	4.72	2.93	4.51	4.16	4.68	1.81	7.66	4.58	2.57	3.79	2.72	3.66	3.20	3.88
Tm	0.694	0.424	0.663	0.604	0.669	0.267	1.10	0.668	0.379	0.551	0.395	0.542	0.472	0.556
Yb	4.41	2.88	4.39	4.02	4.32	1.73	7.06	4.39	2.44	3.52	2.57	3.57	3.09	3.62
Lu	0.615	0.379	0.608	0.560	0.604	0.246	1.00	0.612	0.337	0.494	0.352	0.489	0.428	0.495
Hf	6.72	3.87	6.54	5.61	6.32	1.85	12.4	5.25	3.07	5.01	3.25	4.36	4.01	5.29
Ta	1.84	0.856	1.82	1.33	1.61	0.424	3.40	1.15	0.676	1.21	0.845	1.00	0.922	1.19
Pb	1.59	1.08	1.81	1.21	1.76	0.467	3.03	1.34	0.723	1.21	0.666	1.06	0.986	1.14
Th	2.23	1.21	2.49	1.61	2.72	0.375	4.28	1.49	0.710	1.24	0.784	1.06	1.01	1.56
U	0.692	0.378	0.824	0.478	0.824	0.123	1.36	0.440	0.219	0.404	0.242	0.320	0.295	0.481

(continued)

Table 1: Continued

Sample:	I2114	IB2109	I2113	I2112	I2111	IB2108	I2110	I2108	I2109	IB2106	IB2107	I2105	IB2103	I2106
Latitude (°N):	65.054	65.057	65.055	65.057	65.055	65.053	65.050	65.050	65.055	65.038	65.050	64.911	64.914	64.923
Longitude (°W):	14.958	14.954	14.959	14.960	14.968	14.972	14.993	15.054	15.018	15.064	15.033	15.286	15.287	15.291
Inferred age (Ma):	6.3	6.0	5.7	5.5	5.3	5.1	5.1	4.4	4.4	4.4	4.4	3.0	3.0	2.9
Area:	VII	VIII	VIII	VIII										
<i>Major elements (wt %)</i>														
SiO ₂	49.73	49.26	47.00	48.80	47.44	49.04	47.74	48.62	48.55	49.26	48.93	47.79	48.07	47.80
TiO ₂	3.59	3.84	1.76	3.96	3.70	3.12	2.17	1.78	2.80	1.84	2.90	1.80	2.08	1.61
Al ₂ O ₃	12.77	12.71	15.59	12.91	12.84	13.23	14.12	15.17	13.30	14.69	13.31	14.75	16.02	14.03
Fe ₂ O ₃	4.89	3.85	2.89	5.56	5.14	5.90	4.92	3.76	8.19	2.15	4.80	4.09	4.64	2.77
FeO	9.21	11.07	8.17	9.04	9.54	8.56	7.57	7.46	6.32	9.20	9.57	7.74	6.86	8.76
MnO	0.21	0.23	0.18	0.22	0.23	0.23	0.20	0.19	0.23	0.19	0.23	0.20	0.18	0.19
MgO	4.97	4.97	6.50	5.02	5.57	5.17	7.12	7.27	5.73	7.49	5.90	7.78	5.63	8.00
CaO	9.33	9.20	12.17	9.16	10.13	9.76	11.83	12.92	10.35	12.62	10.53	12.09	12.04	12.30
Na ₂ O	2.78	2.87	2.34	2.77	2.59	2.86	2.22	2.19	2.74	2.25	2.69	2.10	2.37	2.01
K ₂ O	0.82	0.53	0.25	0.55	0.57	0.62	0.29	0.15	0.34	0.20	0.31	0.23	0.19	0.17
P ₂ O ₅	0.40	0.42	0.16	0.46	0.45	0.35	0.21	0.15	0.29	0.16	0.30	0.15	0.21	0.12
H ₂ O ⁺	0.63	0.74	2.89	1.18	1.39	0.87	1.53	0.39	0.66	0.41	0.53	1.40	1.22	1.73
Total	99.35	99.69	99.90	99.63	99.59	99.71	99.92	100.05	99.50	100.47	100.00	100.12	99.51	99.48
<i>Minor and trace elements (μg/g)</i>														
Cr	63.8	53.3	192	52.5	97.3	57.2	237	215	75.3	239	91.2	168	113	356
Ni	40.8	32.9	63.7	33.5	55.9	31.6	52.8	87.0	39.9	76.6	51.2	88.9	47.1	109
Li	6.42	6.23	3.60	5.36	4.95	5.67	4.88	3.98	6.99	3.91	5.91	4.76	4.51	3.72
Be	1.22		0.520	1.22	1.14		0.688				0.985	0.510	0.659	0.403
B	1.24	1.88	0.488	1.13	1.11	0.786	0.322	0.313	0.872	0.425	0.774	0.377	0.265	0.317
Rb	25.9	12.4	2.71	11.0	7.05	11.8	2.63	1.18	6.40	2.16	3.32	3.16	2.01	1.66
Sr	312	327	242	327	302	309	267	216	239	211	229	219	251	150
Y	48.1	52.8	27.0	65.9	46.1	49.1	30.5	28.8	44.0	28.0	44.8	25.6	33.3	25.9
Zr	262	260	97.7	267	259	214	128	91.8	169	94.7	185	86.3	121	74.9
Nb	19.8	19.8	7.64	22.4	20.7	16.9	10.2	6.85	14.2	7.50	15.3	7.70	10.2	5.24
Cs	0.398	0.135	0.782	0.128	0.0601	0.0679	0.0095	0.0091	0.106	0.0127	0.0541	0.0563	0.0085	0.0051
Ba	126	134	43.5	138	134	126	68.6	40.0	84.2	42.9	86.7	50.0	64.3	25.9
La	18.5	19.4	6.79	21.9	19.5	17.1	9.36	6.18	13.1	6.61	13.7	6.80	9.71	4.35
Ce	47.1	51.8	18.5	55.9	50.6	43.4	24.9	16.2	32.9	17.5	34.9	17.6	24.2	11.9
Pr	6.67	7.40	2.70	7.52	7.16	6.04	3.58	2.46	4.74	2.67	4.95	2.65	3.43	1.82
Nd	32.0	35.2	13.1	38.4	34.5	29.4	17.2	12.2	23.3	12.8	24.2	12.7	16.6	9.67
Sm	8.77	9.35	3.67	9.26	8.83	7.66	4.71	3.59	6.42	3.59	6.50	3.52	4.42	2.98
Eu	2.79	3.12	1.34	3.11	2.96	2.64	1.72	1.34	2.21	1.31	2.23	1.40	1.62	1.13
Gd	8.99	9.77	4.20	9.99	9.29	8.45	5.19	4.39	7.23	4.43	7.36	4.12	5.27	3.73
Tb	1.48	1.68	0.737	1.77	1.50	1.38	0.881	0.768	1.23	0.767	1.29	0.727	0.883	0.666
Dy	8.48	9.50	4.49	10.0	8.78	8.06	5.30	4.73	7.43	4.71	7.82	4.49	5.39	4.21
Ho	1.67	1.86	0.948	2.04	1.76	1.64	1.07	1.00	1.56	0.977	1.61	0.934	1.14	0.927
Er	4.07	4.62	2.41	4.94	4.30	4.12	2.79	2.53	3.95	2.56	4.06	2.42	3.06	2.35
Tm	0.585	0.648	0.363	0.721	0.604	0.614	0.402	0.384	0.599	0.369	0.618	0.359	0.432	0.355
Yb	3.72	4.14	2.41	4.79	3.93	3.91	2.56	2.54	3.85	2.46	4.09	2.37	2.86	2.40
Lu	0.507	0.586	0.335	0.638	0.537	0.536	0.365	0.354	0.530	0.346	0.566	0.330	0.402	0.334
Hf	6.71	6.81	2.60	6.83	6.62	5.40	3.35	2.51	4.57	2.56	4.88	2.45	3.19	2.08
Ta	1.44	1.28	0.549	1.64	1.52	1.21	0.724	0.502	0.935	0.504	1.03	0.523	0.736	0.389
Pb	1.27	1.33	0.506	1.52	1.20	1.22	0.620	0.522	0.968	0.530	0.999	0.506	0.684	0.354
Th	1.64	1.75	0.483	2.14	1.63	1.49	0.706	0.524	1.06	0.543	1.13	0.472	0.822	0.321
U	0.550	0.538	0.149	0.704	0.543	0.478	0.185	0.135	0.317	0.159	0.323	0.152	0.261	0.105

(continued)

Table 1: Continued

Sample:	IB2104	I2107	IB2105	I2101	I2102	I2103	I2104	IB2101	IB2102	JB-3	av.	RSD%
Latitude (°N):	64.916	64.941	64.939	64.883	64.884	64.885	64.897	64.881	64.884			
Longitude (°W):	15.289	15.306	15.291	15.381	15.388	15.419	15.371	15.370	15.399	(n=5)		
Inferred age (Ma):	2.9	2.7	2.7	2.0	2.0	2.0	2.0	2.0	2.0			
Area:	VIII											
<i>Major elements (wt %)</i>												
SiO ₂	48.21	49.23	46.81	48.69	49.15	48.87	48.79	46.29	46.36			
TiO ₂	1.63	2.50	2.81	2.22	2.74	2.15	2.70	2.53	4.39			
Al ₂ O ₃	14.15	13.75	14.60	14.29	13.38	13.74	13.32	14.69	13.32			
Fe ₂ O ₃	4.17	2.49	4.21	4.36	3.25	2.79	4.69	2.65	5.58			
FeO	7.37	11.40	9.22	8.55	11.20	9.76	9.72	10.41	10.32			
MnO	0.19	0.23	0.20	0.21	0.23	0.21	0.23	0.20	0.24			
MgO	7.80	6.22	7.16	6.57	5.90	7.08	5.86	8.60	5.32			
CaO	12.05	11.22	10.36	11.63	10.87	12.20	10.75	10.81	9.06			
Na ₂ O	2.06	2.48	2.47	2.37	2.53	2.30	2.45	2.27	2.77			
K ₂ O	0.15	0.27	0.41	0.19	0.28	0.21	0.34	0.24	0.69			
P ₂ O ₅	0.13	0.24	0.27	0.19	0.27	0.20	0.26	0.26	0.51			
H ₂ O ⁺	1.87	0.48	1.19	0.54	0.68	0.93	1.01	0.71	1.71			
Total	99.79	100.49	99.71	99.82	100.48	100.45	100.13	99.65	100.27			
<i>Minor and trace elements (μg/g)</i>												
Cr	314	121	108	139	91.7	197	92.3	294	32.5			
Ni	99.3	55.1	88.4	77.2	56.0	78.9	56.1	175	32.7			
Li	4.56	5.62	4.69	5.61	5.66	4.26	5.21	4.28	5.45	7.20	2.4	
Be	0.428	0.706	0.795		0.815	0.604	0.779	0.603	1.43	0.603	2.1	
B	0.148	0.801	0.809	0.534	0.796	0.594	0.843	0.753	1.04	20.7	0.5	
Rb	1.85	4.50	6.91	2.68	5.48	3.32	6.10	4.19	11.4	15.5	3.8	
Sr	151	171	334	184	196	184	177	277	343	415	1.3	
Y	28.0	39.3	32.7	36.0	46.2	33.0	42.4	31.6	54.0	22.6	2.8	
Zr	82.9	144	150	116	163	119	165	129	273	86.2	1.2	
Nb	5.88	11.8	14.6	9.81	13.0	9.80	13.0	13.1	24.9	1.85	1.0	
Cs	0.0025	0.0426	0.0205	0.0301	0.0520	0.0279	0.0605	0.0411	0.0407	0.935	1.3	
Ba	29.4	49.6	89.9	49.2	56.1	40.7	53.5	67.5	145	239	1.7	
La	5.09	9.28	12.6	8.73	11.4	7.90	10.2	10.6	20.9	8.12	2.3	
Ce	13.8	23.9	31.2	21.9	29.3	21.3	26.5	26.6	53.6	21.5	2.2	
Pr	2.02	3.50	4.28	3.13	4.22	3.12	3.87	3.86	7.45	3.18	1.7	
Nd	10.5	17.3	21.0	15.8	21.1	15.2	19.2	18.7	36.0	15.9	1.6	
Sm	3.20	5.09	5.36	4.41	5.85	4.36	5.60	4.90	8.99	4.17	1.5	
Eu	1.24	1.69	1.93	1.54	2.03	1.60	1.87	1.81	3.23	1.34	2.5	
Gd	3.99	5.72	5.94	5.29	6.98	5.19	6.31	5.31	9.84	4.63	0.9	
Tb	0.720	1.02	0.942	0.943	1.22	0.889	1.12	0.902	1.60	0.755	0.9	
Dy	4.50	6.36	5.65	5.88	7.62	5.59	7.04	5.32	9.13	4.63	2.6	
Ho	0.991	1.37	1.14	1.27	1.62	1.18	1.46	1.08	1.85	0.979	2.4	
Er	2.54	3.58	2.81	3.17	4.22	3.02	3.82	2.75	4.58	2.56	2.0	
Tm	0.383	0.537	0.410	0.498	0.633	0.454	0.579	0.408	0.640	0.387	1.6	
Yb	2.60	3.58	2.59	3.29	4.21	3.10	3.83	2.61	4.13	2.63	2.6	
Lu	0.361	0.509	0.360	0.478	0.598	0.411	0.542	0.361	0.567	0.378	2.3	
Hf	2.29	3.86	3.79	3.16	4.39	3.24	4.35	3.28	6.82	2.65	0.9	
Ta	0.437	0.870	1.04	0.667	0.978	0.742	0.959	0.902	1.76	0.114	1.0	
Pb	0.390	0.646	0.778	0.624	0.839	0.557	0.773	0.613	1.28	5.01	1.6	
Th	0.406	0.725	0.968	0.746	0.916	0.605	0.822	0.672	1.55	1.32	2.2	
U	0.125	0.216	0.346	0.219	0.281	0.201	0.273	0.205	0.498	0.482	1.6	

unleached powders. For some samples, Sr–Nd–Hf isotope measurements were made for both acid-leached and unleached sample powders. Leaching was performed in hot 3M HCl (110°C) for 1 h, and the residual powders were multiply rinsed with water prior to dissolution. In most case, differences between leached and unleached results are within the analytical uncertainties, indicating that there is little or no significant surface contamination (Table 2). All Pb isotope analyses were performed on leached powders. Leaching for Pb isotope analysis was performed in hot 1M HCl (110°C) for 20 min, and then the residues were rinsed several times with water prior to acid digestion. After leaching, 30–80% of the Pb was leached out of the samples. Total procedural blanks (including contamination during pulverizing) for Sr, Nd, Hf and Pb were commonly less than 40, 15, 10, and 30 pg, respectively, and are considered to be negligible with respect to the abundances of the elements in the dissolved samples (more than 30000, 200, 100, and 150 ng for Sr, Nd, Hf, and Pb, respectively). $^{87}\text{Sr}/^{86}\text{Sr}$ ratios of NBS SRM 987 yielded an average of 0.710190 ± 30 (2σ , $n=106$), and the average of $^{143}\text{Nd}/^{144}\text{Nd}$ ratios of La Jolla is 0.511863 ± 20 (2σ , $n=109$), respectively. NBS SRM 987 and La Jolla data were normalized to $^{87}\text{Sr}/^{86}\text{Sr} = 0.710240$ and $^{143}\text{Nd}/^{144}\text{Nd} = 0.511860$, respectively, and these normalization factors are applied to the sample data to facilitate comparison between the datasets. The $^{176}\text{Hf}/^{177}\text{Hf}$ ratios of the JMC475 and JMCl4375 Hf standards yielded averages of 0.282150 ± 6 (2σ , $n=9$) and 0.282187 ± 8 (2σ , $n=24$), respectively, during the course of analysis. To facilitate comparison, all Hf isotope ratios have been normalized to a JMC475 $^{176}\text{Hf}/^{177}\text{Hf} = 0.282160$. The NBS SRM981 Pb standard yielded an average ($n=14$) of $^{206}\text{Pb}/^{204}\text{Pb} = 16.9422 \pm 14$ (2σ), $^{207}\text{Pb}/^{204}\text{Pb} = 15.5000 \pm 13$ (2σ) and $^{208}\text{Pb}/^{204}\text{Pb} = 36.7262 \pm 44$ (2σ), respectively, during the same analytical campaign; these values agree well with those obtained by Kuritani & Nakamura (2003) ($^{206}\text{Pb}/^{204}\text{Pb} = 16.9424$, $^{207}\text{Pb}/^{204}\text{Pb} = 15.5003$, $^{208}\text{Pb}/^{204}\text{Pb} = 36.7266$) and are comparable to those from other studies (e.g. Baker *et al.*, 2004). Typical analytical reproducibilities (2σ) for the samples are about 40 ppm for Sr and Nd, and 30 ppm for Hf isotope analyses, and those for $^{206}\text{Pb}/^{204}\text{Pb}$, $^{207}\text{Pb}/^{204}\text{Pb}$ and $^{208}\text{Pb}/^{204}\text{Pb}$ are less than 150 ppm. All isotope ratios presented in Table 2 are not age-corrected. Age correction does not significantly change the Sr–Nd–Hf isotope data, and thus we have used the measured Sr–Nd–Hf isotope data throughout. The maximum age correction for Pb isotope ratios is -0.054 (2900 ppm) for $^{206}\text{Pb}/^{204}\text{Pb}$, -0.003 (160 ppm) for $^{207}\text{Pb}/^{204}\text{Pb}$ and -0.057 (1500 ppm) for $^{208}\text{Pb}/^{204}\text{Pb}$, respectively, calculated using Pb–Th–U concentrations and the inferred age of the samples. These correction factors are clearly larger than the analytical errors, except for $^{207}\text{Pb}/^{204}\text{Pb}$. Thus, we have used the age-corrected Pb isotope data throughout.

RESULTS

Major and trace element compositions

Using the alkali–silica classification (Irvine & Baragar, 1971) the Tertiary lavas from eastern Iceland are mostly tholeiitic basalts and basaltic andesites. They are also classified as tholeiitic series lavas (no normative nepheline) based on their CIPW normative composition (Yoder & Tilley, 1962), except for two samples, IB1609 and IB1610, which have very minor ($<1.4\%$) amounts of normative nepheline ($\text{Fe}^{3+}/\text{Fe}_{\text{total}}$ molar ratio = 0.12 is used in the calculation). The major element compositions of these samples fall within the ranges reported for Tertiary lavas from Iceland (Wood, 1976, 1978; Hardarson *et al.*, 1997). Figure 2 shows variation diagrams for selected major and minor elements plotted against MgO content. The MgO contents range from 2.6 to 8.6 wt %, and show broad positive correlations with Al_2O_3 , CaO, Cr and Ni, and negative correlations with SiO_2 and Na_2O . The compositional trends of the lavas from the Thingmuli volcanic center, which are believed to lie on a single liquid line of descent related by crystal fractionation (Carmichael, 1964), are also shown for comparison. The Thingmuli trends generally track the data of this study, suggesting that the eastern Iceland Tertiary lavas are related, to a first order, by fractional crystallization. Samples with MgO of >7 wt % show distinct trends: the older lavas (13–11.5 and 9–7 Ma periods) have lower SiO_2 , CaO and Cr, and higher Al_2O_3 , Na_2O and Ni contents at a given MgO content than those of the younger lavas (~ 5 –2 Ma). It should be noted that there is almost no sign of accumulation of phenocrysts in most lava samples based on petrographic observations.

Primitive mantle normalized trace element patterns of the samples are illustrated together with those of the postglacial lavas in Fig. 3. Variations in the Tertiary lavas are smaller than those of the postglacial lavas and the patterns are similar to those of the postglacial tholeiitic lavas. In most of the Tertiary lavas, Ba is slightly enriched compared with its neighbouring elements Rb and Th [$2 \times \text{Ba}_N / (\text{Rb}_N + \text{Th}_N) = 1.33 \pm 0.30$ (1σ) (excluding two lavas showing plagioclase accumulation); subscript N denotes primitive mantle normalization], a feature shared with the postglacial lavas. On the other hand, the Tertiary lavas (with MgO >7 wt %) have no apparent positive Sr anomaly, which is normally observed in the trace element patterns of Icelandic basalts [$2 \times \text{Sr}_N / (\text{Pr}_N + \text{Nd}_N) = 1.05 \pm 0.16$ (1σ)]. The differentiated lavas (MgO <7 wt %) show negative Sr anomalies [$2 \times \text{Sr}_N / (\text{Pr}_N + \text{Nd}_N) = 0.72 \pm 0.21$ (1σ)], indicating fractionation of plagioclase. Temporal variations in trace element compositions are described in a subsequent section.

Sr–Nd–Hf–Pb isotope compositions

The $^{87}\text{Sr}/^{86}\text{Sr}$ and ϵ_{Nd} values of the lavas analyzed in this study range from 0.70313 to 0.70349 and from 6.7

Table 2: *Sr, Nd, Hf and Pb isotope data for the Tertiary lavas from eastern Iceland*

Sample	$^{87}\text{Sr}/^{86}\text{Sr}$	$^{143}\text{Nd}/^{144}\text{Nd}$	$^{176}\text{Hf}/^{177}\text{Hf}$	$^{206}\text{Pb}/^{204}\text{Pb}$	$^{207}\text{Pb}/^{204}\text{Pb}$	$^{208}\text{Pb}/^{204}\text{Pb}$
I1301	0.703294	0.513023	0.283195	18.5351	15.4825	38.2265
I1302	0.703323	0.513011	0.283192	18.5313	15.4819	38.2213
I1303	0.703326	0.513051	0.283185	18.5531	15.4785	38.2174
I1304	0.703307	0.513030	0.283176	18.5965	15.4855	38.2677
I1305	0.703253	0.513016	0.283178	18.5275	15.4845	38.2153
I1306	0.703339	0.513004	0.283149	18.5635	15.4878	38.2603
I1307	0.703339	0.513010	0.283154	18.6125	15.4878	38.2894
I1308	0.703379	0.512991	0.283175	18.4344	15.4867	38.1752
I1309	0.703323	0.513003	0.283144	18.7062	15.5004	38.3901
I1310	0.703395	0.513011	0.283145	18.6498	15.4889	38.3118
I1311	0.703291	0.513029	0.283149	18.6450	15.4915	38.3248
I1312	0.703318	0.513002	0.283151	18.6611	15.4906	38.3301
I1313	0.703309	0.513053	0.283146	18.6433	15.4869	38.3116
I1314	0.703300	0.513008	0.283152	18.6339	15.4887	38.3041
I1315	0.703384	0.513007	0.283146	18.6594	15.4875	38.3213
I1401	0.703375	0.513031	0.283171	18.5902	15.4847	38.2000
I1402	0.703364	0.513046	0.283185	18.4649	15.4714	38.1033
I1403	0.703341	0.513035	0.283185	18.5575	15.4811	38.2403
I1404	0.703398	0.513013	0.283150	18.5817	15.4846	38.2577
I1405	0.703315	0.513045	0.283152	18.6812	15.4912	38.3483
I1406	0.703254	0.513032	0.283169	18.5865	15.4875	38.2610
I1407	0.703267	0.513016	0.283158	18.6051	15.4883	38.3119
I1408	0.703245	0.513034	0.283151	18.5851	15.4830	38.2797
I1409	0.703298	0.513015	0.283148	18.6378	15.4893	38.3463
I1410	0.703319	0.513021	0.283155	18.6168	15.4852	38.3177
I1411	0.703286	0.513017	0.283152	18.6033	15.4897	38.3164
I1412	0.703394	0.513013	0.283157	18.5192	15.4856	38.2296
I1413	0.703450	0.513010	0.283139	18.5907	15.4811	38.2478
I1413 leached	0.703422	0.513002	0.283136			
I1414	0.703444	0.513003	0.283160	18.4798	15.4778	38.1955
I1415	0.703345	0.513020	0.283189	18.3359	15.4656	38.0353
I1416	0.703401	0.513012	0.283170	18.4375	15.4853	38.1938
I1417	0.703285	0.513017	0.283176	18.4029	15.4713	38.0973
I1418	0.703328	0.513006	0.283164	18.2575	15.4589	37.9825
I1418 duplicate				18.2568	15.4583	37.9819
IB1401	0.703322	0.512992	0.283153	18.4446	15.4675	38.1400
IB1402	0.703247	0.513012	0.283150	18.6577	15.4877	38.3553
IB1403	0.703237	0.513015	0.283149	18.6716	15.4880	38.3676
IB1404	0.703362	0.513032	0.283155	18.6060	15.4870	38.3123
IB1405	0.703395	0.512989	0.283151	18.4879	15.4848	38.2157
IB1406	0.703368	0.513008	0.283170	18.4441	15.4736	38.1462
I1501	0.703449	0.512979	0.283178	18.3421	15.4817	38.1684
I1502	0.703468	0.512993	0.283179	18.3462	15.4796	38.1666
I1503	0.703462	0.512996	0.283204	18.2400	15.4752	38.0983
I1503 duplicate				18.2391	15.4733	38.0936
I1504	0.703364	0.512993	0.283189	18.2692	15.4724	38.0904
I1505	0.703313	0.513013	0.283188	18.2217	15.4718	38.0143
I1505 leached	0.703346	0.513009	0.283184	18.2846	15.4718	38.0755

(continued)

Table 2: *Continued*

Sample	$^{87}\text{Sr}/^{86}\text{Sr}$	$^{143}\text{Nd}/^{144}\text{Nd}$	$^{176}\text{Hf}/^{177}\text{Hf}$	$^{206}\text{Pb}/^{204}\text{Pb}$	$^{207}\text{Pb}/^{204}\text{Pb}$	$^{208}\text{Pb}/^{204}\text{Pb}$
I1507	0.703373	0.513022	0.283183	18.3514	15.4748	38.1287
I1508	0.703377	0.513028	0.283173	18.3318	15.4705	38.0873
I1509	0.703389	0.513025	0.283174	18.4052	15.4782	38.1546
I1510	0.703369	0.513014	0.283177	18.3597	15.4722	38.1155
I1601	0.703309	0.513046	0.283213	18.2668	15.4695	37.9869
I1602	0.703300	0.513036	0.283218	18.2740	15.4716	37.9982
I1603	0.703358	0.512990	0.283187	18.2742	15.4713	38.0497
I1604	0.703290	0.513045	0.283229	18.2134	15.4653	37.9272
I1605	0.703323	0.513010	0.283198	18.2072	15.4648	37.9942
I1606	0.703330	0.513030	0.283209	18.2178	15.4675	38.0029
I1607	0.703357	0.513030	0.283205	18.2207	15.4739	38.0386
I1608	0.703390	0.512996	0.283185	18.2961	15.4703	38.0818
IB1601	0.703357	0.513021	0.283165	18.4498	15.4809	38.1814
IB1602	0.703373	0.513022	0.283174	18.4614	15.4782	38.1918
IB1603	0.703379	0.513018	0.283165	18.5037	15.4811	38.2214
IB1604	0.703367	0.513015	0.283171	18.5004	15.4827	38.2237
IB1605	0.703371	0.513022	0.283187	18.3865	15.4752	38.1484
IB1606	0.703350	0.513033	0.283175	18.3848	15.4738	38.1275
IB1607	0.703343	0.513010	0.283172	18.3600	15.4756	38.1104
IB1607 leached	0.703318		0.283174			
IB1608	0.703350	0.513032	0.283169	18.4232	15.4735	38.1564
IB1609	0.703277	0.513059	0.283238	18.1393	15.4582	37.8952
IB1610	0.703252	0.513034	0.283238	18.1583	15.4607	37.9207
I2101	0.703137	0.513067	0.283187	18.4940	15.4547	38.1561
I2102	0.703222	0.513040	0.283178	18.4435	15.4607	38.1362
I2103	0.703223	0.513054	0.283177	18.4418	15.4583	38.1342
I2104	0.703186	0.513033	0.283184	18.4472	15.4641	38.1452
I2105	0.703150	0.513087	0.283207	18.4117	15.4663	38.0841
I2106	0.703133	0.513074	0.283205	18.3830	15.4455	38.0624
I2107	0.703179	0.513071	0.283187	18.4315	15.4579	38.1220
I2108	0.703153	0.513070	0.283176	18.4590	15.4659	38.1550
I2109	0.703176	0.513048	0.283171	18.4990	15.4704	38.1613
I2110	0.703200	0.513053	0.283176	18.4578	15.4749	38.1213
I2111	0.703225	0.513047	0.283141	18.5186	15.4782	38.1785
I2112	0.703207	0.513050	0.283146	18.5242	15.4803	38.1934
I2113	0.703161	0.513086	0.283193	18.3692	15.4591	37.9986
I2114	0.703182	0.513043	0.283140	18.5503	15.4795	38.2078
I2115	0.703311	0.513048	0.283161	18.5017	15.4780	38.1750
I2116	0.703246	0.513023	0.283199	18.2459	15.4602	37.9744
I2117	0.703357	0.513034	0.283158	18.6051	15.4753	38.2301
I2118	0.703254	0.513035	0.283168	18.4269	15.4742	38.1241
IB2101	0.703210	0.513021	0.283152	18.4868	15.4794	38.1912
IB2102	0.703234	0.513060	0.283145	18.4408	15.4748	38.1440
IB2103	0.703182	0.513050	0.283176	18.4994	15.4703	38.1632
IB2104	0.703207	0.513039	0.283189	18.3825	15.4415	38.0473
IB2105	0.703279	0.513018	0.283141	18.5100	15.4877	38.2329
IB2106	0.703197	0.513051	0.283168	18.4705	15.4633	38.1534
IB2107	0.703147	0.513064	0.283177	18.4842	15.4701	38.1502
IB2108	0.703213	0.513024	0.283154	18.4727	15.4763	38.1412
IB2109	0.703193	0.513065	0.283145	18.5368	15.4817	38.2030

Table 2: *Continued*

Sample	$^{87}\text{Sr}/^{86}\text{Sr}$	$^{143}\text{Nd}/^{144}\text{Nd}$	$^{176}\text{Hf}/^{177}\text{Hf}$	$^{206}\text{Pb}/^{204}\text{Pb}$	$^{207}\text{Pb}/^{204}\text{Pb}$	$^{208}\text{Pb}/^{204}\text{Pb}$
IB2110	0.703277	0.513015	0.283179	18.2530	15.4624	37.9954
I2201	0.703369	0.513005	0.283171	18.3846	15.4766	38.1371
I2202	0.703258	0.513055	0.283145	18.5343	15.4837	38.2085
I2203	0.703283	0.513060	0.283144	18.5361	15.4783	38.1975
I2204	0.703382	0.512992	0.283157	18.4816	15.4812	38.2453
I2205	0.703375	0.513017	0.283209	18.2865	15.4689	38.0607
I2206	0.703308	0.513050	0.283167	18.4799	15.4723	38.1490
I2207	0.703308	0.513032	0.283156	18.4378	15.4636	38.0987
I2208	0.703306	0.513009	0.283151	18.6732	15.5001	38.3628
I2209	0.703430	0.513011	0.283186	18.3752	15.4763	38.1194
I2210	0.703252	0.513008	0.283146	18.4209	15.4577	38.0992
I2210 duplicate				18.4198	15.4554	38.0897
I2211	0.703300	0.513013	0.283138	18.4390	15.4564	38.1175
I2212	0.703411	0.513001	0.283175	18.5192	15.4812	38.1771
I2213	0.703286	0.513040	0.283154	18.4362	15.4681	38.1235
IB2201	0.703345	0.513004	0.283173	18.3468	15.4727	38.1066
IB2202	0.703293	0.513013	0.283159	18.5115	15.4814	38.2399
IB2203	0.703489	0.513016	0.283165	18.5590	15.4848	38.2158
IB2203 leached	0.703451	0.513028				
IB2204	0.703326	0.513016	0.283145	18.6275	15.4925	38.3401
IB2205	0.703309	0.513033	0.283155	18.4036	15.4608	38.0884
IB2206	0.703324	0.513035	0.283147	18.4412	15.4562	38.1142

All isotope data are not age corrected. Average values of internal precision (2σ) for $^{87}\text{Sr}/^{86}\text{Sr}$, $^{143}\text{Nd}/^{144}\text{Nd}$ and $^{176}\text{Hf}/^{177}\text{Hf}$ are ± 0.000008 , ± 0.000005 and ± 0.000004 , respectively.

to 8.8, respectively; the data define a broad negative correlation in Sr–Nd isotope space (Fig. 4). Our data fall in the intermediate part of the Sr–Nd isotope array defined by the postglacial basalts. Marked differences in Sr–Nd isotope compositions within the Tertiary lavas from eastern Iceland are observed between lavas older than and younger than c. 6.5 Ma: lavas older than c. 6.5 Ma have higher $^{87}\text{Sr}/^{86}\text{Sr}$ and lower ε_{Nd} than lavas younger than c. 6.5 Ma. The ε_{Hf} values of the Tertiary lavas in this study range between 12.9 and 16.5, within the range of the postglacial lavas ($\varepsilon_{\text{Hf}} = 11.2\text{--}19.5$). The Tertiary Icelandic lavas do not define a single linear trend on the Nd–Hf isotope correlation diagram (Fig. 5). The lavas older than 12 Ma have higher ε_{Hf} values at a given ε_{Nd} than the others, and most lavas of this older period plot above the oceanic basalt regression line of Vervoort *et al.* (1999) (mantle array in Fig. 5). Most of the lavas younger than 12 Ma plot on and around this line. The Tertiary lavas from eastern Iceland cover a range in Pb isotope composition (age corrected), from 18.10 to 18.67 for $^{206}\text{Pb}/^{204}\text{Pb}$, 15.44 to 15.50 for $^{207}\text{Pb}/^{204}\text{Pb}$ and 37.85 to 38.35 for $^{208}\text{Pb}/^{204}\text{Pb}$, all within the range for the postglacial lavas ($^{206}\text{Pb}/^{204}\text{Pb} = 17.92\text{--}19.30$, $^{207}\text{Pb}/^{204}\text{Pb} = 15.41\text{--}15.56$, and $^{208}\text{Pb}/^{204}\text{Pb} =$

37.54–38.93) (Fig. 6). The variations in Pb isotope ratios of the Tertiary lavas are consistent with the range previously reported for lavas from eastern Iceland (Hanam & Schilling, 1997).

Temporal variations in trace element and isotopic compositions

Trace element and Sr–Nd–Hf–Pb isotope ratios of the Tertiary lavas from eastern Iceland show systematic temporal fluctuations; the data from this study have been supplemented with additional data obtained by previous workers (Fig. 7). The $(\text{La}/\text{Sm})_n$, Ba/Nb and Sr–Nd–Hf–Pb isotope ratios of the Tertiary lavas show the following relationships: (1) $(\text{La}/\text{Sm})_n$ shows a constant broad range from 13 to 6.5 Ma [$(\text{La}/\text{Sm})_n = 1.3\text{--}2.0$] with lower ratios (~ 1.2) at around 10 Ma, followed by an abrupt decrease at 6.5 Ma (0.9–1.5); (2) Ba/Nb shows a broad trend of decrease from 13 to 2 Ma with two small positive peaks around 9–8 and 6.5 Ma; (3) $^{87}\text{Sr}/^{86}\text{Sr}$ and ε_{Nd} display abrupt changes at c. 6.5 Ma (lower $^{87}\text{Sr}/^{86}\text{Sr}$ and higher ε_{Nd} at < 6.5 Ma); (4) ε_{Hf} broadly decreases from 13 to 7.5 Ma followed by an increase from 7.5 to 6.5 Ma, with no systematic change after 6.5 Ma; (5) $^{206}\text{Pb}/^{204}\text{Pb}$ and $^{208}\text{Pb}/^{204}\text{Pb}$ broadly

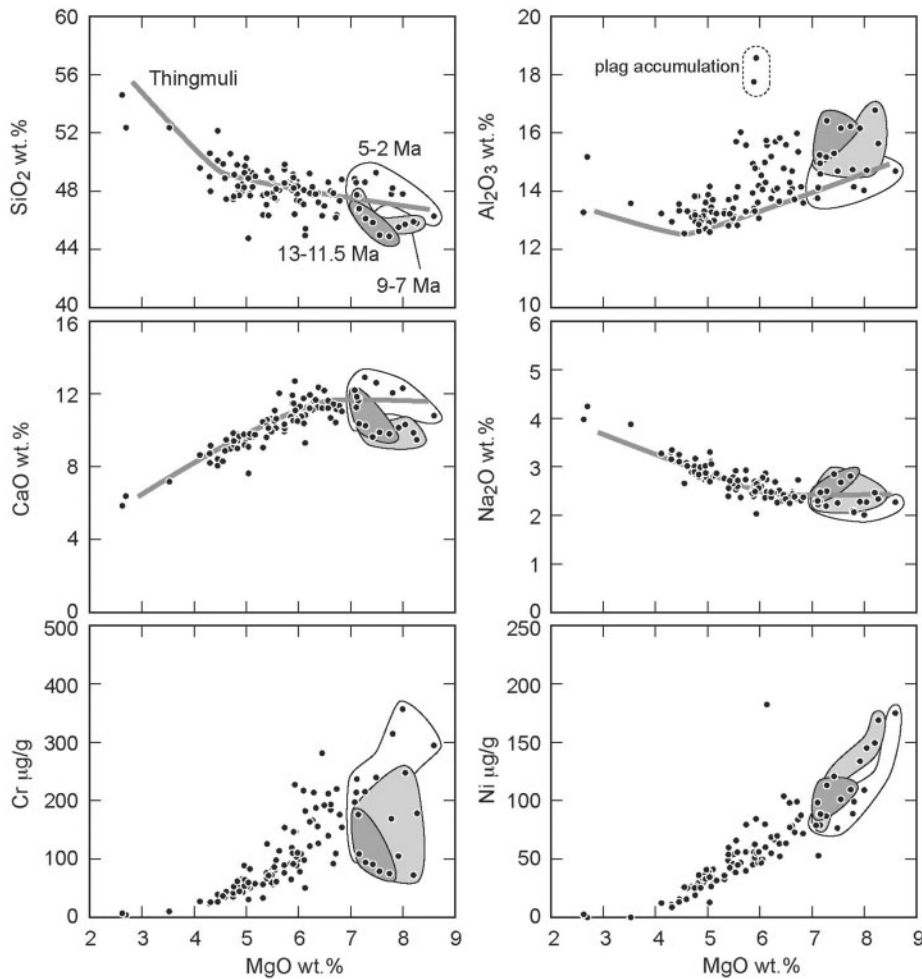


Fig. 2. Major (SiO_2 , Al_2O_3 , CaO and Na_2O) and minor (Cr and Ni) element variations in the Tertiary Icelandic lavas plotted against MgO . The bold lines indicate the trend of Thingmuli lavas (Carmichael, 1964). Fields are also shown for lavas with $\text{MgO} > 7$ wt % from the periods 13–11.5 Ma (dark gray), 9–7 Ma (pale gray) and 5–2 Ma (white). Two samples with high Al_2O_3 content (Il4l5 and Il602) show porphyritic textures with 26–35 vol. % plagioclase phenocrysts.

increase from 13 to 8–7 Ma, and then decrease to 6.5 Ma; there are no systematic temporal changes in the lavas younger than 6.5 Ma; (6) $^{207}\text{Pb}/^{204}\text{Pb}$ also shows a broad increase from 13 to 7.5 Ma with lower ratios (~ 15.46) around 10 Ma, and a decrease from 7.5 to 6.5 Ma. There is also no systematic temporal variation in the lavas younger than 6.5 Ma, which show a wide range of variation from 15.44 to 15.49.

Regression analysis of Pb isotope trends

The Pb isotope data for the lavas from each area (I–VIII and Lagarfljót) (Fig. 1) are plotted separately on Pb isotope diagrams in Fig. 8. The aim here is to see the Pb isotope compositions sequentially and evaluate the secular changes in trends using two-dimensional isotope representations. The 13–11 Ma lavas (areas I–III) generally have lower $^{206}\text{Pb}/^{204}\text{Pb}$ values, and higher $^{207}\text{Pb}/^{204}\text{Pb}$ and

$^{208}\text{Pb}/^{204}\text{Pb}$ at a given $^{206}\text{Pb}/^{204}\text{Pb}$, and thus have higher $\Delta 7/4$ and $\Delta 8/4$ [Δ units indicate vertical deviations from the Northern Hemisphere Reference Line or NHRL (Hart, 1984)]. At 10 Ma (lavas from area IV), the Pb isotope compositions change to $\Delta 7/4$ and $\Delta 8/4$ slightly lower than those of the older lavas. The 10–7.5 Ma lavas (IV and V), therefore, form slightly steeper trends relative to the area I–III lavas. The 7.5–6.5 Ma lavas (VI and Lagarfljót) have similar slopes to those of the trends for the 13–11 Ma lavas. After 6.5 Ma, lavas from areas VII and VIII show steeper trends than those for lavas older than 6.5 Ma.

At first glance, there is a distinction in slopes between the trends formed by the older lavas and those younger than 6.5 Ma. To evaluate this inference more rigorously, we apply the *F*-test to the residual variances of the best-fit regression lines in the Pb isotope plots. This test

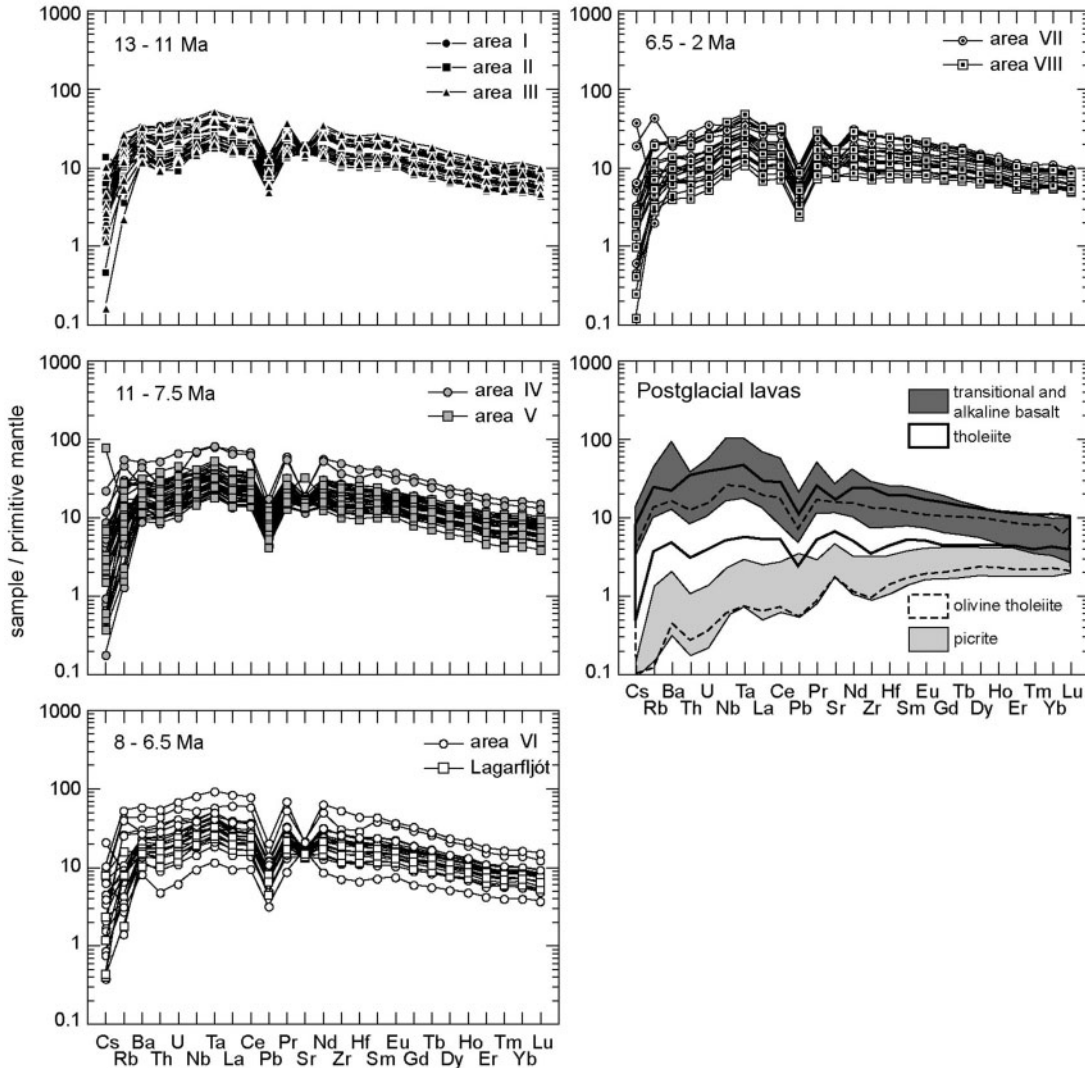


Fig. 3. Primitive mantle normalized trace element patterns for the Tertiary lavas and postglacial Icelandic basalts (Hemond *et al.*, 1993; Chauvel & Hémond, 2000; Skovgaard *et al.*, 2000; Stracke *et al.*, 2003b; Kokfelt *et al.*, 2006). Primitive mantle values from McDonough & Sun (1995).

demonstrates whether the Pb isotope trend can be grouped into several distinct trends or not. First, the Pb isotope population is divided into two subpopulations, older and younger than 6.5 Ma, respectively. In applying the *F*-test, we frame the null hypothesis that the two Pb isotope regression trends can be regarded as the same. If the residual variances of the individual regressions are lower than that of the regression by pooling all data, the two regression lines are different from each other. Table 3 shows the results of the *F*-test performed on the Tertiary Icelandic lavas analyzed in this study. Comparison of the combined residual sum of squares for individual regressions with a pooled regression results in the statistic *F* value of 33.7 and 10.9 for $^{206}\text{Pb}/^{204}\text{Pb}$ – $^{207}\text{Pb}/^{204}\text{Pb}$ and $^{206}\text{Pb}/^{204}\text{Pb}$ – $^{208}\text{Pb}/^{204}\text{Pb}$ relationships, respectively. These values are much greater than the critical *F* value at 1%

(*F*=4.80) and even 0.1% (*F*=7.36) significance levels. The probabilities of *F* values of 33.7 and 10.9 are 4×10^{-10} and $5 \times 10^{-3}\%$, respectively. Therefore, the null hypothesis that the two subpopulations yield the same regression line can be rejected at much better than 99% confidence, providing strong confirmation that there are at least two distinct Pb isotope trends in the Tertiary lavas rather than a single trend.

DISCUSSION

Source characteristics

Statistical examination of the mixing end-member components

To assess the number of end-member components in the source of the Tertiary Icelandic lavas, we used

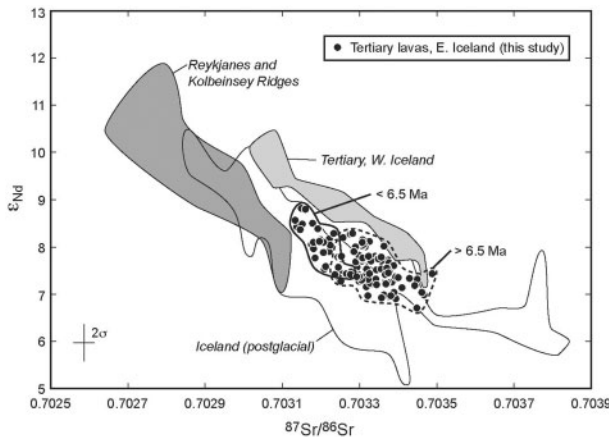


Fig. 4. Correlation between $^{87}\text{Sr}/^{86}\text{Sr}$ and ϵ_{Nd} in the Tertiary lavas of this study compared with variations previously reported for the Tertiary and postglacial Icelandic basalts (Hemond *et al.*, 1993; Hardarson *et al.*, 1997; Stecher *et al.*, 1999; Prestvik *et al.*, 2001; Stracke *et al.*, 2003b; Thirlwall *et al.*, 2004; Kokfelt *et al.*, 2006) and Reykjanes and Kolbeinsey Ridge basalts (Schilling *et al.*, 1999; Thirlwall *et al.*, 2004).

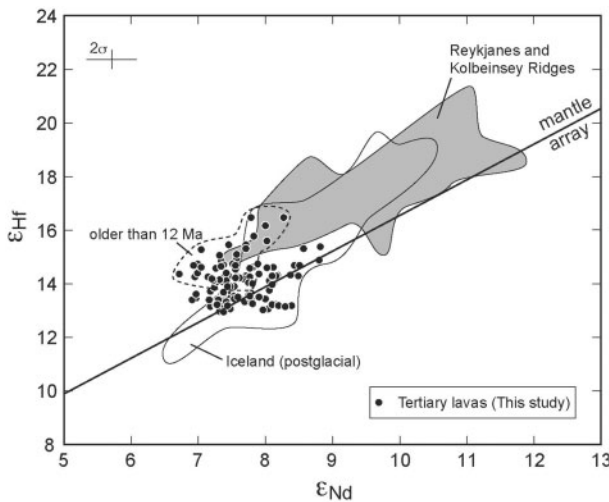


Fig. 5. ϵ_{Nd} vs ϵ_{Hf} isotope correlation diagram for the Tertiary (this study) and postglacial Icelandic lavas (Hanhan *et al.*, 2000; Kempton *et al.*, 2000; Stracke *et al.*, 2003b; Blichert-Toft *et al.*, 2005), and Reykjanes and Kolbeinsey Ridge basalts (Taylor *et al.*, 1997; Schilling *et al.*, 1999; Kempton *et al.*, 2000; Blichert-Toft *et al.*, 2005). The mantle array represents the regression line for all Nd–Hf isotope data for oceanic basalts (Vervoort *et al.*, 1999).

principal component analysis (PCA) on the Pb isotope data. These data have the useful property that the three isotope ratios ($^{206}\text{Pb}/^{204}\text{Pb}$, $^{207}\text{Pb}/^{204}\text{Pb}$ and $^{208}\text{Pb}/^{204}\text{Pb}$) have an identical denominator isotope (i.e. ^{204}Pb), and thus binary mixing between two end-members is expected to form linear arrays in Pb–Pb isotope space; deviations of the data from such an array imply a contribution from a third end-member component. The calculated eigenvectors

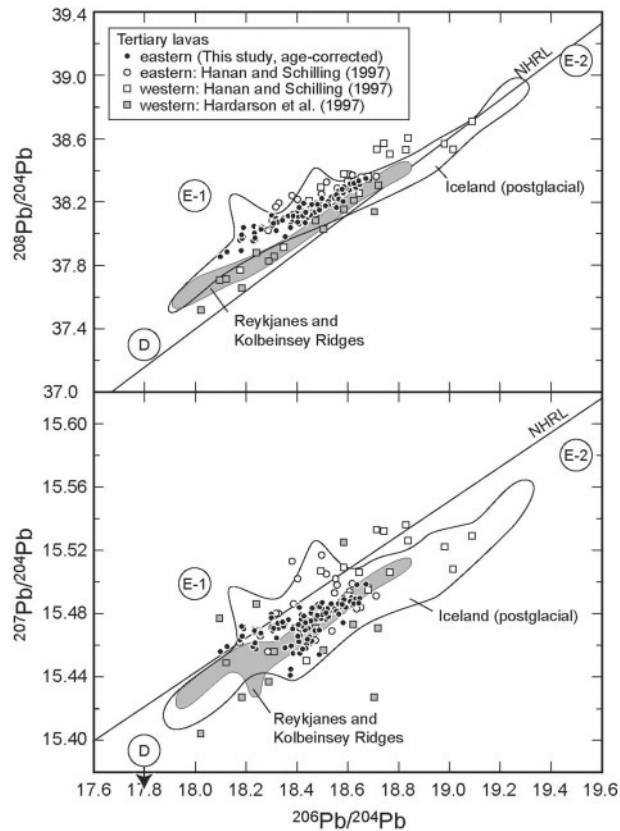


Fig. 6. $^{208}\text{Pb}/^{204}\text{Pb}$ and $^{207}\text{Pb}/^{204}\text{Pb}$ vs $^{206}\text{Pb}/^{204}\text{Pb}$ variation diagrams for the Tertiary lavas of this study and from the literature (Hanhan & Schilling, 1997; Hardarson *et al.*, 1997), and for postglacial lavas from submarine Iceland and the Reykjanes and Kolbeinsey Ridges (Baker *et al.*, 2004; Thirlwall *et al.*, 2004; Kokfelt *et al.*, 2006). NHRL, Northern Hemisphere Reference Line (Hart, 1984). The circled fields labeled E-1, E-2 and D are the hypothetical end-member components for the Tertiary Icelandic lavas defined in this study (Table 4). Error bars for Pb isotope ratios are within the scale of the symbols.

in the PCA may thus provide useful information for identifying the number of end-member mixing components in the source of the basalts. In contrast, PCA results for multiple isotope systems often indicate the spurious influence of a third or fourth end-member component because of differences in the denominator elements, as pointed out by Blichert-Toft *et al.* (2005) and Debaille *et al.* (2006). Figure 9 shows the PCA output for the Pb isotope data. The three eigenvectors (v_1 , v_2 , and v_3) account for 86.86%, 12.05% and 1.09%, respectively, of the variance in the dataset. Because the first two principal eigenvectors (v_1 and v_2) represent 98.91% of the total variance, the contribution of v_3 is probably negligible. The result of this PCA justifies the use of a mixing model involving three end-member components. Pb isotope data for lavas from eastern Iceland reported by Hanhan & Schilling (1997) were also plotted using the projection vectors of our dataset (Fig. 9). Some of their data deviate greatly from the first

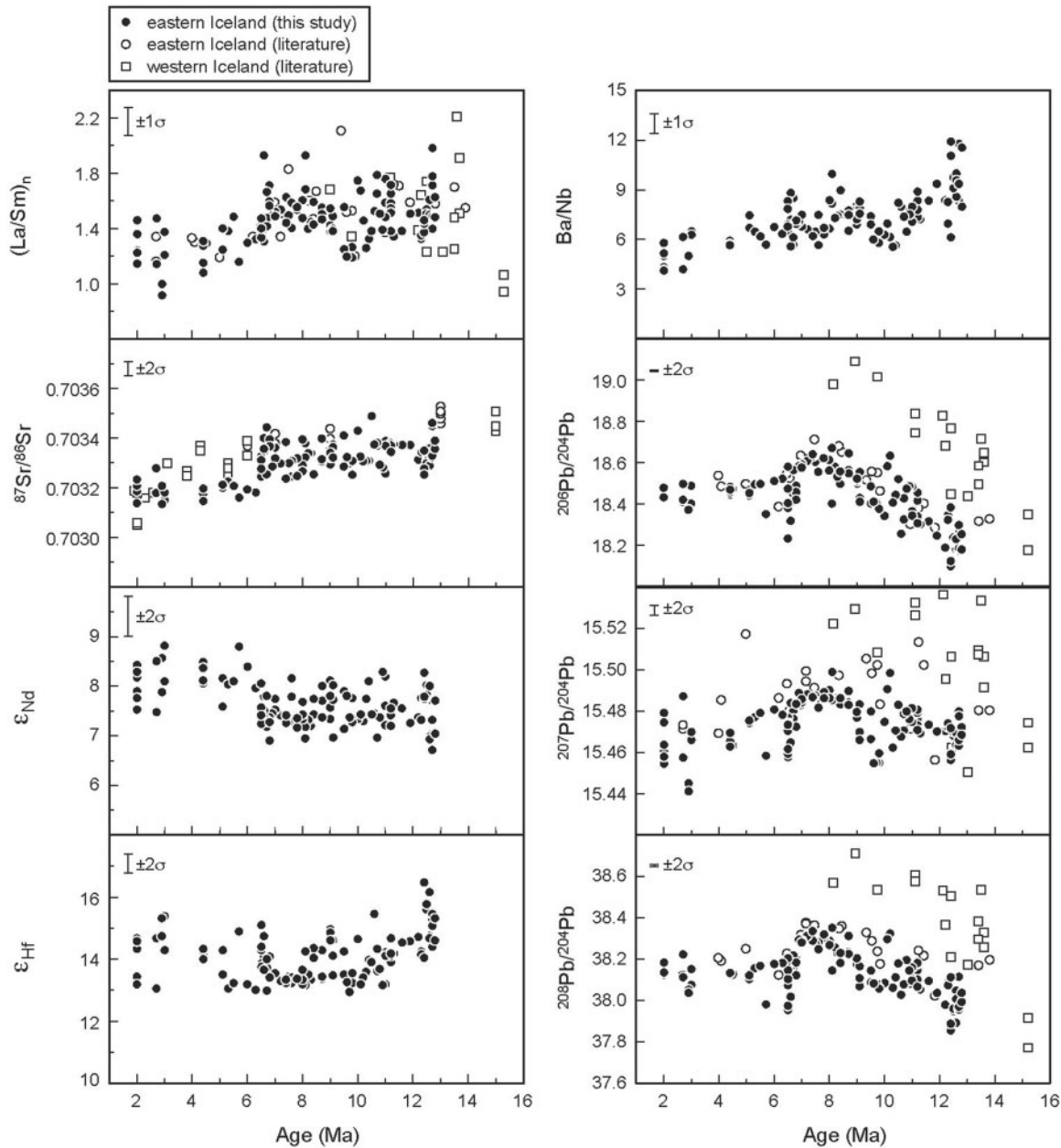


Fig. 7. Temporal variations in $(\text{La}/\text{Sm})_n$, Ba/Nb and Sr–Nd–Hf–Pb isotope ratios of the Tertiary lavas from eastern and western Iceland obtained in this study and from the literature (O’Nions & Pankhurst, 1973; Schilling *et al.*, 1982; Hanan & Schilling, 1997). $(\text{La}/\text{Sm})_n$ is calculated using the chondrite values of Anders & Grevesse (1989). Error bars indicate the typical analytical uncertainties: 1σ for trace element ratios and 2σ for isotope ratios.

principal eigenvector towards the $^{207}\text{Pb}/^{204}\text{Pb}$ axis, presumably because of some analytical problem (see below).

We also applied PCA to the Pb isotope data for the post-glacial Icelandic lavas and Reykjanes and Kolbeinsey Ridge basalts combined with those of the Tertiary lavas from this study (Fig. 10). First, we performed PCA on the Pb isotope data obtained by the double-spike (DS) method (Baker *et al.*, 2004; Thirlwall *et al.*, 2004). Then data obtained by conventional TIMS and Tl-corrected

MC-ICP-MS methods were also projected using the projection vectors of the DS-corrected Pb isotope data. Our dataset is also shown plotted onto the plane containing the two calculated eigenvectors. The contribution of the first principal eigenvector, v_1 , increases significantly (to 98.51%), because the variation in $^{206}\text{Pb}/^{204}\text{Pb}$ (17.9–19.3) relative to $^{207}\text{Pb}/^{204}\text{Pb}$ and $^{208}\text{Pb}/^{204}\text{Pb}$ of the postglacial lavas is larger than that in the Tertiary lavas (18.1–18.7) (Fig. 6). The second and third eigenvectors (v_2 and v_3) account for

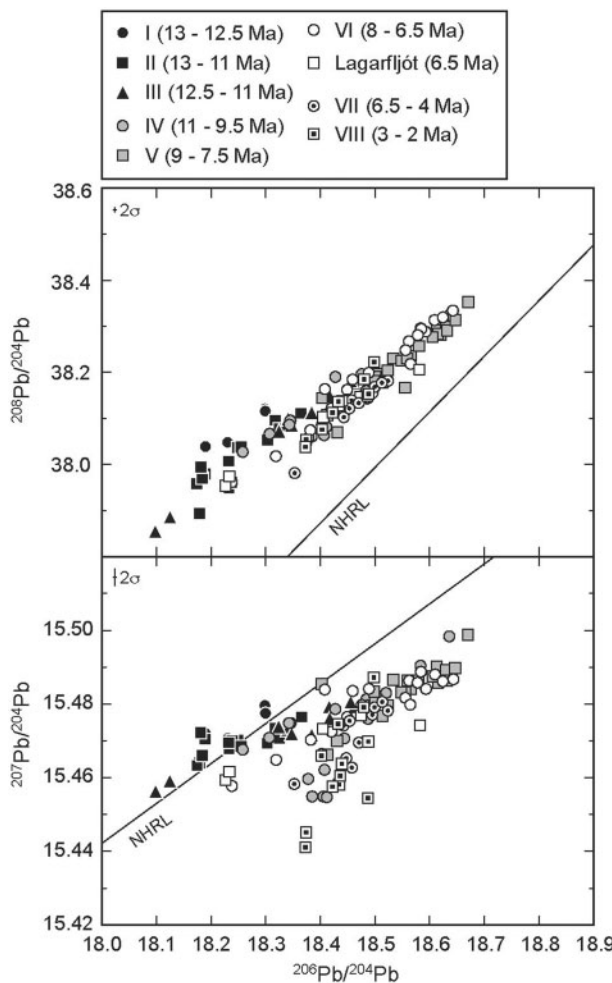


Fig. 8. Pb isotope variation diagrams showing the sequential changes within the eastern Iceland Tertiary successions. The samples are divided into nine groups based on the sampling locality, as indicated in Fig. 1.

1.13 and 0.36%, respectively, of the variance. The cumulative contribution of v_1 and v_2 yields over 99.5% of the data variance. Therefore, the PCA results provide a strong confirmation that the Pb isotope variations in the sub-aerial lavas from Iceland (Tertiary and postglacial) and adjacent mid-ocean ridges can be well approximated by a single plane in $^{206}\text{Pb}/^{204}\text{Pb}$ - $^{207}\text{Pb}/^{204}\text{Pb}$ - $^{208}\text{Pb}/^{204}\text{Pb}$ three-dimensional space, thus confirming mixing between three mantle end-member components. The projection of the data produced by the conventional and, to a lesser extent, the Tl-doping method show some scatter and some of the data deviate considerably from the v_1 - v_2 plane towards the $^{207}\text{Pb}/^{204}\text{Pb}$ axis (Fig. 10b and c). This may be due to an inadequate mass fractionation correction to the Pb isotope data measured by the conventional and Tl-doping methods (Baker *et al.*, 2004, 2005; Thirlwall *et al.*, 2004).

The marked difference in the Pb isotope arrays can be seen in plots of v_1 vs v_2 (Figs 9a and 10a). The v_1 eigenvector lies roughly along the radiogenic extension of the Pb isotope trend, and could be considered to largely reflect the involvement of an end-member with the most radiogenic Pb isotope composition. The v_2 eigenvector defines the offset among the data arrays and varies mostly in the direction of $^{207}\text{Pb}/^{204}\text{Pb}$ (Figs 9c and 10c); v_2 thus appears to be dominantly controlled by the involvement of an end-member with higher ΔTh .

Geochemical characteristics of the end-member components

The three mantle end-member components required to explain the isotopic compositions of the Icelandic basalts are termed here E-1 (enriched-1), E-2 (enriched-2), and D (depleted), respectively; these are analogous to the Pb isotope end-members 'e', 'p' and 'd' proposed by Hanan & Schilling (1997).

Table 3: F-test statistics of the Pb isotope regression trends for Tertiary Icelandic lavas

	Number of samples	Degree of freedom	Residual sum of squares (RSS)		F-statistic		Null hypothesis probability level (P) %	
			RSS*	RSS†	F^*	$F^†$	P^*	$P^†$
Pooled	114	112	0.0073918	0.1255726				
Older than 6.5 Ma	91	89	0.0032800	0.0953901				
Younger than 6.5 Ma	23	21	0.0013048	0.0094769				
Combined		110	0.0045848	0.1048670				
Difference between pooled and combined		2	0.0028070	0.0207057	33.67	10.86	4×10^{-10}	0.005

* RSS, F and P calculated for $^{206}\text{Pb}/^{204}\text{Pb}$ - $^{207}\text{Pb}/^{204}\text{Pb}$ relationship.

† RSS, F and P calculated for $^{206}\text{Pb}/^{204}\text{Pb}$ - $^{208}\text{Pb}/^{204}\text{Pb}$ relationship.

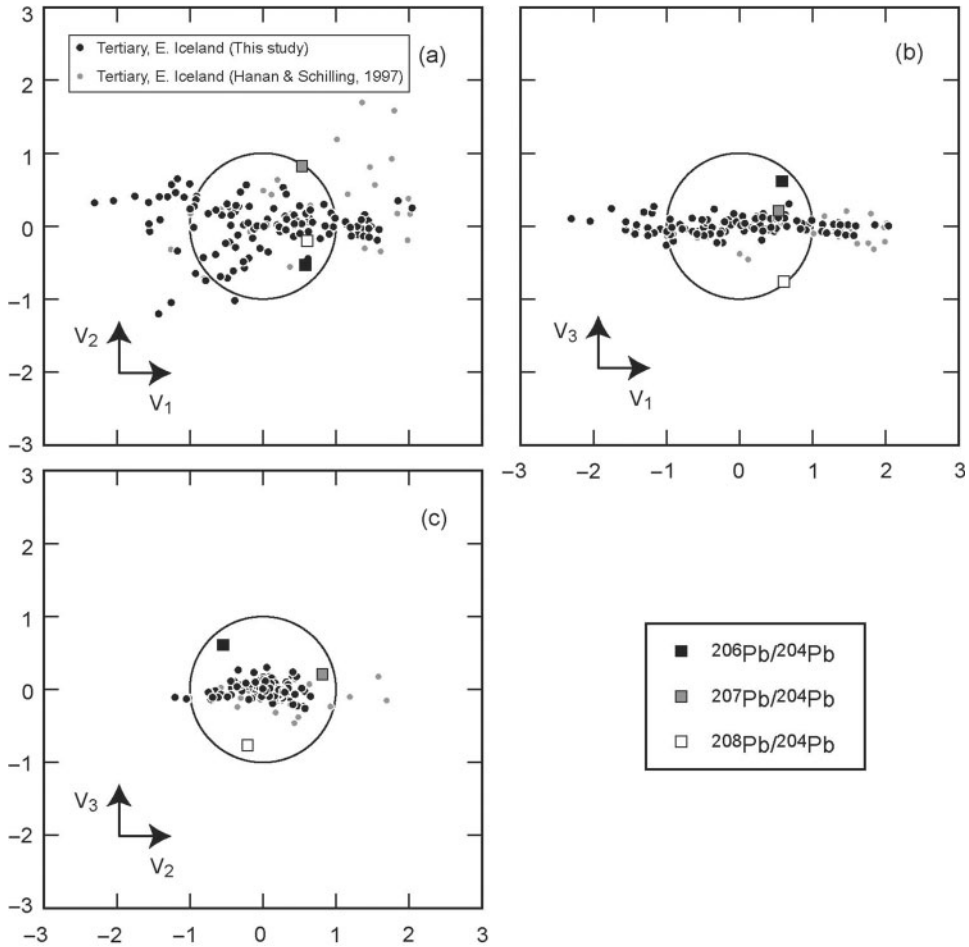


Fig. 9. Results of principal component analysis (PCA) of the Pb isotope compositions of the Tertiary Icelandic lavas, calculated using $^{206}\text{Pb}/^{204}\text{Pb}$, $^{207}\text{Pb}/^{204}\text{Pb}$ and $^{208}\text{Pb}/^{204}\text{Pb}$ data as raw variables. Principal component scores for each of the eigenvectors are plotted in the planes containing two principal eigenvectors: (a) v_1 and v_2 , (b) v_1 and v_3 , and (c) v_2 and v_3 , respectively. The circles of unit radius represent 1σ standard deviation of the variations in the dataset along each eigenvector after normalization, and the arithmetic means are located at the centers of each circle. Pb isotope data for Tertiary lavas from eastern Iceland by Hanan & Schilling (1997) are projected using the projection vectors calculated for the Pb isotope data of this study.

The E-1 end-member component largely contributes to the 12–13 Ma lavas and has lower $^{206}\text{Pb}/^{204}\text{Pb}$ and higher $\Delta 7/4$ and $\Delta 8/4$ than the E-2 end-member component (Figs 6 and 11). Hf isotope compositions also discriminate between the E-1 and E-2 end-member components: E-1 has more radiogenic $^{176}\text{Hf}/^{177}\text{Hf}$ ($\Delta\epsilon_{\text{Hf}}$) than E-2 (Fig. 11). The Sr–Nd–Pb isotope signature of the E-1 end-member component is characteristic of an Enriched Mantle 1 (EM-1) type mantle source (see Zindler & Hart, 1986). Thirlwall *et al.* (2004) also reported postglacial Icelandic basalts characterized by higher $\Delta 7/4$ (3.5), $\Delta 8/4$ (62) and $^{87}\text{Sr}/^{86}\text{Sr}$ (0.7034), and lower ϵ_{Nd} (7.9), which appear to have a greater contribution from the E-1 end-member component. This end-member component is also considered to contribute largely to the postglacial off-axis central volcano Öraefajökull, whose magmas are characterized by high $^{87}\text{Sr}/^{86}\text{Sr}$ (0.7037) and low ϵ_{Nd} (\sim 7–6) (Prestvik

et al., 2001; Thirlwall *et al.*, 2004; Kokfelt *et al.*, 2006). The >12 Ma lavas also have higher Ba/Nb, Pb/Nb and ϵ_{Hf} for a given ϵ_{Nd} (i.e. high $\Delta\epsilon_{\text{Hf}}$) (Figs 5 and 11). These features are commonly observed in hotspot lavas belonging to the typical EM-1 group; for example, Hawaii (Blichert-Toft *et al.*, 1999) and Pitcairn (Eisele *et al.*, 2002). Higher $\Delta\epsilon_{\text{Hf}}$ is attributed to higher Lu/Hf for a given Sm/Nd in the source of the E-1 end-member component. A plausible explanation for the higher $\Delta\epsilon_{\text{Hf}}$ is selective fractionation of specific Hf-rich minerals, such as zircon or rutile, in the original source material. Selective fractionation of appropriate minerals could take place during the sedimentary cycle between sand and clay fractions (Patchett *et al.*, 1984; Plank & Langmuir, 1998) or be associated with crustal differentiation by anatexis during high-grade metamorphic reactions (Schmitz *et al.*, 2004). Therefore, two possible candidates for the origin of the E-1 end-member

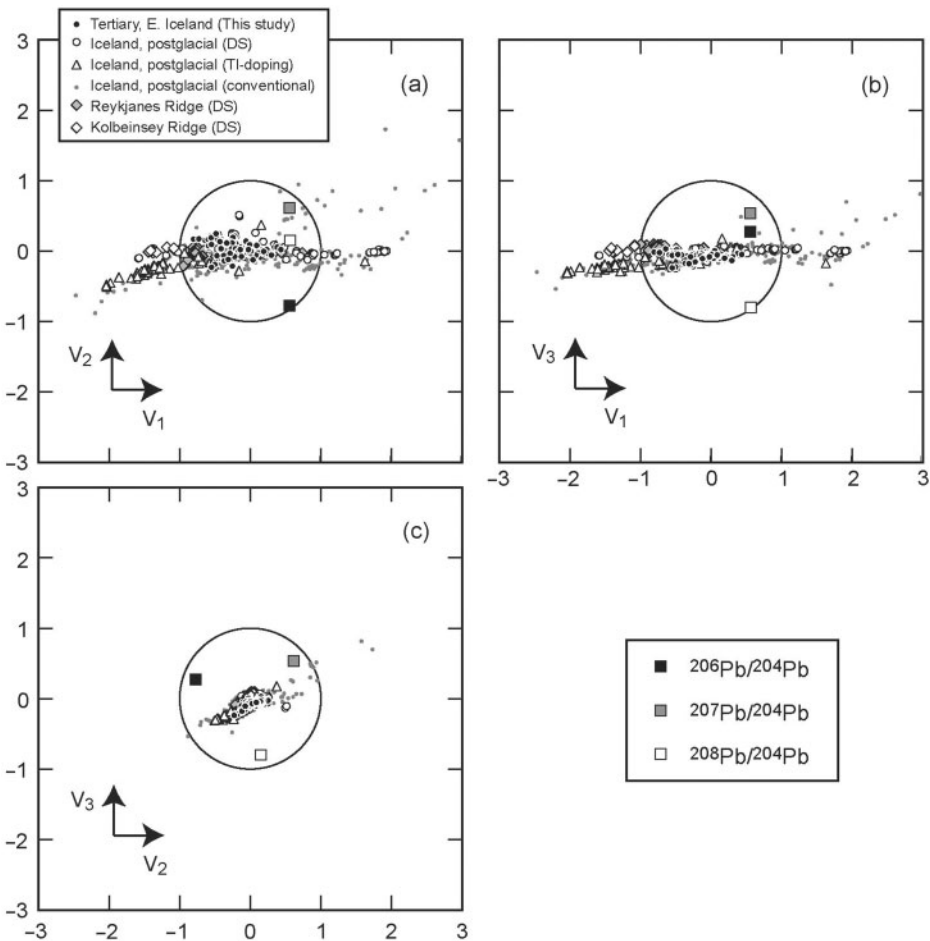


Fig. 10. PCA results for postglacial Icelandic lavas and Reykjanes and Kolbeinsey Ridge basalts. The eigenvectors are calculated using DS Pb isotope data (Baker *et al.*, 2004; Thirlwall *et al.*, 2004): (a) v_1 and v_2 , (b) v_1 and v_3 , and (c) v_2 and v_3 , respectively. Data for postglacial lavas analyzed by Tl-normalized MC-ICP-MS (Kempton *et al.*, 2000; Stracke *et al.*, 2003b) and conventional TIMS method (Welke *et al.*, 1968; Sun & Jahn, 1975; Sun *et al.*, 1975; Elliott *et al.*, 1991; Hards *et al.*, 1995, 2000; Stecher *et al.*, 1999; Chauvel & Hémond, 2000; Prestvik *et al.*, 2000; Breddam, 2002; Kokfelt *et al.*, 2006) and those of this study (DS method) are also projected using the projection vectors.

component can be proposed: pelagic sediments and lower crustal mafic granulites. Both candidates are able to explain the Sr–Nd–Pb isotope characteristics of the E-1 end-member component based on the parent/daughter element ratios in these isotope systems observed in appropriate crustal lithologies (e.g. Rudnick & Goldstein, 1990; Rudnick & Fountain, 1995; Plank & Langmuir, 1998; Eisele *et al.*, 2002). Higher Ba/Nb and Pb/Nb are also diagnostic of continental-derived materials in the source of the E-1 end-member, because both sediments and continental crustal materials show strong enrichments in Ba and Pb and depletion in Nb (e.g. Rudnick & Fountain, 1995; Plank & Langmuir, 1998; Eisele *et al.*, 2002). Hanan *et al.* (2004) have recently proposed that lower continental crust is the most plausible candidate for the EM-1 or Dupal-type source component in Southeast Indian Ridge basalts with high $\Delta\epsilon_{\text{Hf}}$. Thus one candidate for the origin of this

end-member component is consistent with that proposed by Hanan *et al.* (2004).

The E-2 end-member component is obvious in the most radiogenic Pb isotope and least radiogenic Hf isotope compositions of the 7–8 Ma lavas analyzed in this study. The 7–8 Ma lavas have $^{87}\text{Sr}/^{86}\text{Sr}$ and ϵ_{Nd} values comparable with those of lavas erupted before 12 Ma (Figs 7 and 11). More radiogenic Pb isotope compositions are observed in the postglacial Icelandic lavas, which are mostly alkali basalts erupted either in the southwestern rift (e.g. Hekla and Torfajökull) or in the off-axis regions (e.g. Snæfellsnes Peninsula and Vestmannaeyjar) in Iceland (e.g. Stecher *et al.*, 1999; Thirlwall *et al.*, 2004; Kokfelt *et al.*, 2006). The E-2 end-member component is thus most clearly identified in the postglacial alkaline lavas and must have $^{206}\text{Pb}/^{204}\text{Pb} > 19.3$, $^{207}\text{Pb}/^{204}\text{Pb} > 15.56$, and $^{208}\text{Pb}/^{204}\text{Pb} > 38.9$. This interpretation is supported by the PCA. The direction of

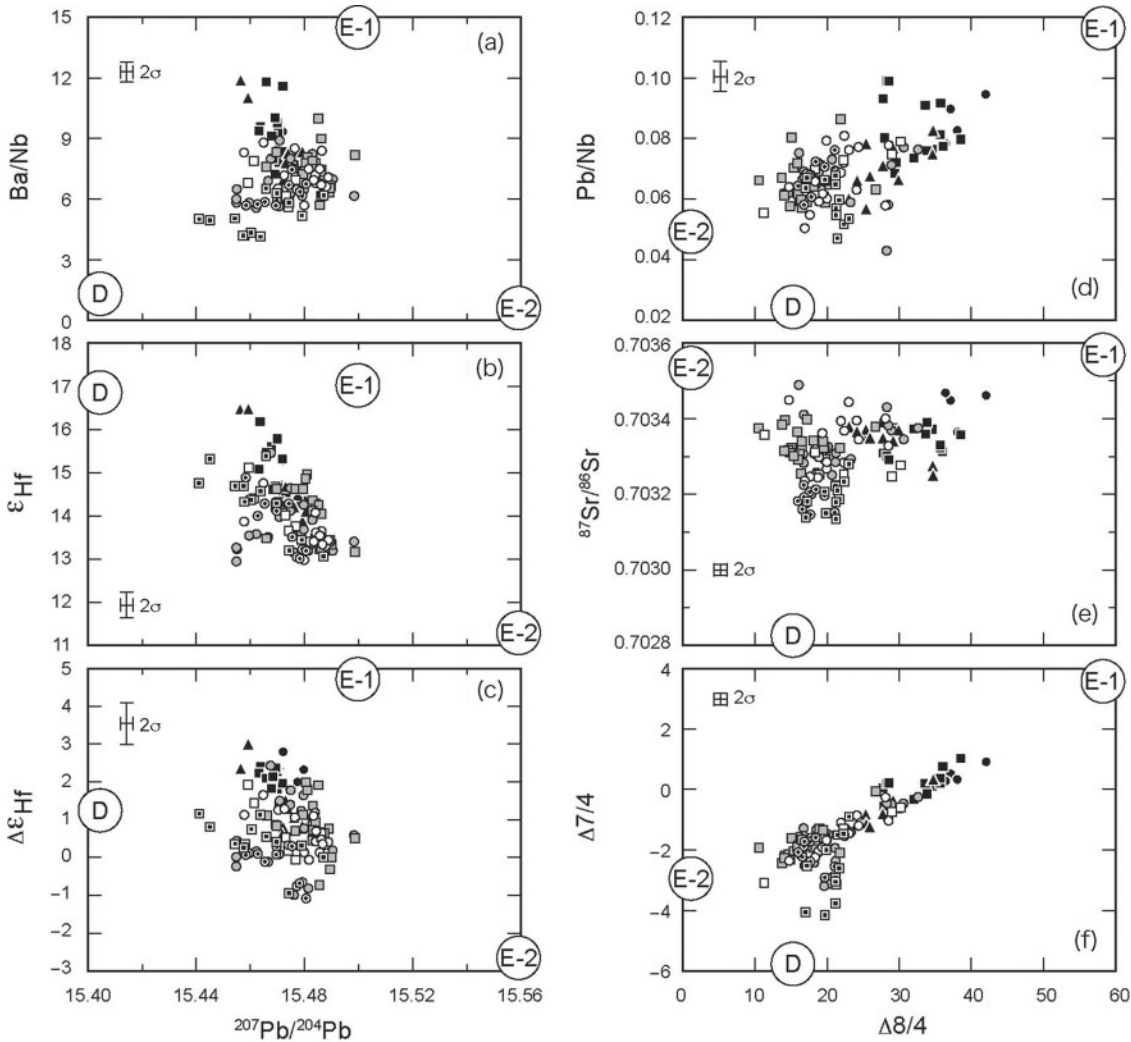


Fig. 11. Variation diagram showing correlations between the trace element and Sr–Hf–Pb isotope compositions of the Tertiary Icelandic lavas. (a) $^{207}\text{Pb}/^{204}\text{Pb}$ vs Ba/Nb, (b) $^{207}\text{Pb}/^{204}\text{Pb}$ vs ϵ_{Hf} , (c) $^{207}\text{Pb}/^{204}\text{Pb}$ vs $\Delta\epsilon_{\text{Hf}}$, (d) $\Delta 8/4$ vs Pb/Nb, (e) $\Delta 8/4$ vs $^{87}\text{Sr}/^{86}\text{Sr}$, and (f) $\Delta 8/4$ vs $\Delta 7/4$. The compositions of possible end-member components (or melts derived from them) are also shown as the circled field labeled E-1, E-2 and D, respectively. Symbols are the same as in Fig. 8. Error bars show 2σ uncertainties both for trace element and isotopic compositions.

the first principal eigenvector (v_1) defined by the Tertiary lavas (Fig. 9) is almost identical to that defined by both Tertiary and postglacial Icelandic lavas (Fig. 10). The composition of the E-2 end-member should plot at the higher extension along the v_1 vector (Fig. 10a). The radiogenic Pb isotope ratios indicate long-term higher U/Pb and Th/Pb in the E-2 end-member than in the other end-member components. Such higher ratios can be produced by fractionation as a result of extraction of Pb from the original source material. For example, preferential loss of Pb could occur during dehydration of subducted oceanic crust in subduction zones (e.g. Ayers, 1998). The lower Ba/Nb of the E-2 end-member can also be explained by recycling of dehydrated oceanic crust as a result of selective loss of Ba relative to Nb during dehydration (e.g. Stalder *et al.*, 1998).

On the other hand, higher $^{87}\text{Sr}/^{86}\text{Sr}$ (>0.7034) for the proposed E-2 end-member component may imply that such a process did not significantly change the Rb/Sr ratio (Fig. 11). The oceanic crust also has lower Lu/Hf and Sm/Nd than the residual mantle and dehydration processes seem to have little effect on these ratios (e.g. Stracke *et al.*, 2003a). Thus, the oceanic crust can also be a possible candidate for the Nd–Hf isotope signature of the E-2 end-member (low $^{143}\text{Nd}/^{144}\text{Nd}$ – $^{176}\text{Hf}/^{177}\text{Hf}$). The isotopic characteristics of the E-2 end-member component, described above, are similar to those of mantle components previously called ‘FOZO’ or ‘C’ (Hanhan & Graham, 1996; Hanan *et al.*, 2004; Stracke *et al.*, 2005), and are postulated to be due to the recycling of oceanic crust (Hanhan & Graham, 1996; Stracke *et al.*, 2005).

The D end-member component is most prominent in the <6.5 Ma magmatism relative to other periods. The <6.5 Ma lavas are depleted in incompatible elements, with lower $(\text{La}/\text{Sm})_n$ and Ba/Nb than the older lavas (Figs 7 and 11). The $^{87}\text{Sr}/^{86}\text{Sr}$ and ε_{Nd} of the <6.5 Ma lavas are the least and most radiogenic, respectively; that is, these lavas are geochemically the most depleted among the Tertiary lavas from eastern Iceland (Figs 4 and 11). The D end-member component is lower in $^{207}\text{Pb}/^{204}\text{Pb}$ than the other two end-member components (Fig. 6). This end-member component also contributes to the incompatible element depleted lavas in the Neovolcanic Zone and the Reykjanes and Kolbeinsey Ridges (Figs 4–6). The Tertiary lavas <6.5 Myr old are similar to the Reykjanes Ridge basalts; both are characterized by a negative principal component score for the Pb isotope second eigenvector (v_2) (Fig. 10), implying that the D end-member component is similar to that contributing to the ocean-ridge basalts; that is, depleted mid-ocean ridge basalt (MORB) mantle (DMM). Although this end-member component is likely to be peridotitic material depleted by ancient melt extraction, there are two hypotheses for the origin of this source: (1) ambient MORB source mantle (e.g. Schilling, 1973; Mertz *et al.*, 1991; Hanan & Schilling, 1997; Mertz & Haase, 1997; Stracke *et al.*, 2003b) or (2) ancient recycled oceanic lithosphere, which has been inferred to be an intrinsic component of the Iceland mantle plume (e.g. Fitton *et al.*, 1997, 2003; Chauvel & Hémond, 2000; Skovgaard *et al.*, 2000; Kokfelt *et al.*, 2006). It should be noted that evaluation of the origin of the D end-member component is not the aim of this study. Our dataset does not provide new constraints on this end-member component, because there are no Tertiary Icelandic lavas with depleted geochemical and isotopic compositions similar to the postglacial primitive tholeiitic basalts. We, therefore, simply note that the D end-member is likely to be peridotitic material that was depleted in incompatible elements by ancient melt extraction.

Origin of temporal geochemical variations in the eastern Iceland Tertiary lavas

Estimation of relative contributions from the three end-member components

We have calculated the elemental Pb fraction from the three end-member components using two-dimensional isotope space representations ($^{206}\text{Pb}/^{204}\text{Pb}$ vs $^{207}\text{Pb}/^{204}\text{Pb}$ and $^{206}\text{Pb}/^{204}\text{Pb}$ vs $^{208}\text{Pb}/^{204}\text{Pb}$), following the method described by Schilling *et al.* (2003). The Pb isotope compositions of the three end-member components for the ternary mixing model are shown in Fig. 6 and in Table 4. Before calculation we checked the applicability of the Pb isotope compositions of the three end-members using PCA and confirmed that these mostly plot on the plane defined by the Pb isotope compositions of Icelandic lavas

Table 4. Pb isotope compositions of the proposed end-member components used in the mixing model

	End-member component		
	E-1	E-2	D
$^{206}\text{Pb}/^{204}\text{Pb}$	18.00	19.50	17.80
$^{207}\text{Pb}/^{204}\text{Pb}$	15.50	15.58	15.36
$^{208}\text{Pb}/^{204}\text{Pb}$	38.25	39.10	37.30

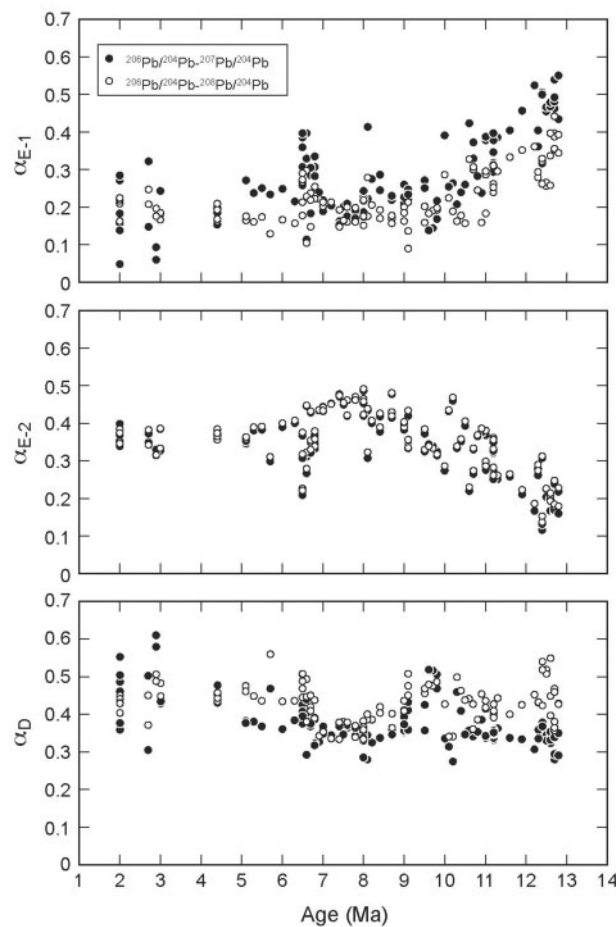


Fig. 12. Temporal variations in contributions from the three end-member components, E-1, E-2 and D, respectively, represented by elemental Pb fractions ($\alpha_{\text{E-1}}$, $\alpha_{\text{E-2}}$ and α_{D}).

in the 3-D Pb isotope correlation space based on the fact that the first and second principal components account for 99% of the total variance. Figure 12 shows the temporal variations in elemental Pb fractions from each of the three end-member components.

The contribution of elemental Pb from the E-1 end-member component gradually decreases from ~50% at

13 Ma to ~20% at around 8–7 Ma, and then increases to ~40% immediately before 6.5 Ma, followed by a decrease to ~20–30% at c. 6.5 Ma. The influence of the E-2 end-member component increases from 13 to 8–7 Ma (from 20 to 50%) and subsequently decreased to ~20–40% at c. 6.5 Ma. The contributions of both the E-1 and E-2 end-member components show no systematic secular changes during the period younger than 6.5 Ma. The contribution of the D end-member is more clearly shown by the Pb elemental fraction calculated based on the $^{206}\text{Pb}/^{204}\text{Pb}$ – $^{207}\text{Pb}/^{204}\text{Pb}$ correlation relative to those from $^{206}\text{Pb}/^{204}\text{Pb}$ – $^{208}\text{Pb}/^{204}\text{Pb}$. The contribution from the D end-member component increased to 50% at c. 10 Ma and to 50–60% during the period younger than 6.5 Ma. The temporal trends obtained in this study are essentially similar to those calculated by Hanan & Schilling (1997), confirming our estimations of mixing proportions.

Evaluation of ‘temporal’ variations in Icelandic magmatism

Although the temporal changes in the contributions from the three end-member components can account for geochemical variations in the Tertiary lavas analyzed as part of this study, it is important to realize that the data are confined to the lava piles of eastern Iceland and therefore inevitably give a biased view of the temporal variation in Icelandic magmatism as a whole. Additionally, the postglacial Icelandic lavas show greater variations in geochemical and isotopic compositions than the Tertiary lavas and there are systematic geochemical differences within each volcanic zone (i.e. northern, eastern and western volcanic zones) (e.g. Stracke *et al.*, 2003b; Thirlwall *et al.*, 2004; Kokfelt *et al.*, 2006). These differences presumably reflect lateral heterogeneity in the mantle and may also be due to variations in plume–ridge configuration. The geochemical diversity in the Tertiary lavas can presumably be related to lateral geochemical variations in the mantle source that have existed consistently from the Tertiary to the present; that is, the bulk composition of the Icelandic mantle source has been in a steady state for a few tens of million years. For example, Barker *et al.* (2006) attributed the sequential Nd and Pb isotope variations in the East Greenland lava formations (56.1–55.0 Ma; Storey *et al.*, 2007a, 2007b) to lateral heterogeneity in the proto-Iceland mantle plume tapped by partial melting processes. Below we discuss this issue to examine the ‘temporal’ variations in the compositions of the Tertiary Icelandic lavas.

In Iceland, Tertiary lavas occur on both the eastern and western sides of the current rift axis. Previous studies have revealed clear secular variations in the rare earth element (REE) and Sr–Pb isotope compositions of the Tertiary lavas from both sides (O’Nions & Pankhurst, 1973; Schilling *et al.*, 1982; Hanan & Schilling, 1997; Hanan *et al.*, 2000). The majority of samples analysed in these studies were collected from profiles sampled for paleomagnetic studies (e.g. Dagley *et al.*, 1967;

McDougall *et al.*, 1977, 1984). Although breaks of over 50 km exist in some of these composite sections, the Sr and Pb isotope data for Tertiary lavas from western Iceland (O’Nions & Pankhurst, 1973; Hanan & Schilling, 1997) show temporal trends similar or parallel to those of the lavas from eastern Iceland (Fig. 7). These observations may indicate that regular temporal variations in the geochemical characteristics of the magmatism existed over the whole of Iceland, suggesting a systematic secular change in the source of all Icelandic magmatism, rather than variations in the tapping processes of a laterally heterogeneous source alone. The similarities between the temporal variations in $(\text{La}/\text{Sm})_n$ of lavas from the Tertiary Iceland successions and from the Faeroe Islands (50–60 Ma) (Schilling & Noe-Nygaard, 1974) also seemingly demonstrate that there is a regular secular variation in the (proto-)Icelandic magmatism. In summary, the geochemical variations in the Tertiary lavas probably reflect a true secular variation in Icelandic magmatism. However, it is still difficult to estimate the effect of lateral heterogeneity in the mantle on secular variation in Icelandic magmatism. To advance our knowledge of such secular variation, detailed geochemical studies of the Tertiary lavas from the broad region must be carried out.

Secular changes in mantle composition or post-emplacement processes?

Processes other than secular changes in the mantle composition could lead to systematic variations in magma composition with time. For example, rift relocation and subsequent crustal accretion processes could disturb the preservation of old lavas, casting doubt on the interpretation of the compositional changes observed in the Tertiary lavas as a ‘temporal’ effect [see Hardarson & Fitton (1997) and Hardarson *et al.* (1997)]. Hardarson and coworkers attributed the much smaller range of variation in Nb/Zr of the Tertiary lavas relative to the postglacial lavas to biased sampling, resulting from the subsidence and burial of volumetrically smaller, more geochemically heterogeneous flows. The volumetrically dominant flows with homogeneous compositions erupted and flowed away from the rift axis, and these lavas remain in the upper portion of the crustal section exposed by glacial erosion. Wood *et al.* (1976) interpreted the REE variations in the Tertiary lavas as having been caused by secondary alteration. However, it seems unlikely that either model can be used exclusively to explain the geochemical variations of the Tertiary lavas for the following reasons: (1) Hf isotope compositions, which are thought to be unaffected by secondary alteration or weak metamorphism (e.g. Wood *et al.*, 1976), show systematic temporal variations and correlations with other trace element and isotope ratios (Figs 7 and 11); (2) it seems difficult to explain the correlation between geochemical fluctuations and geological and geophysical observations (discussed in the following section), by subsidence and

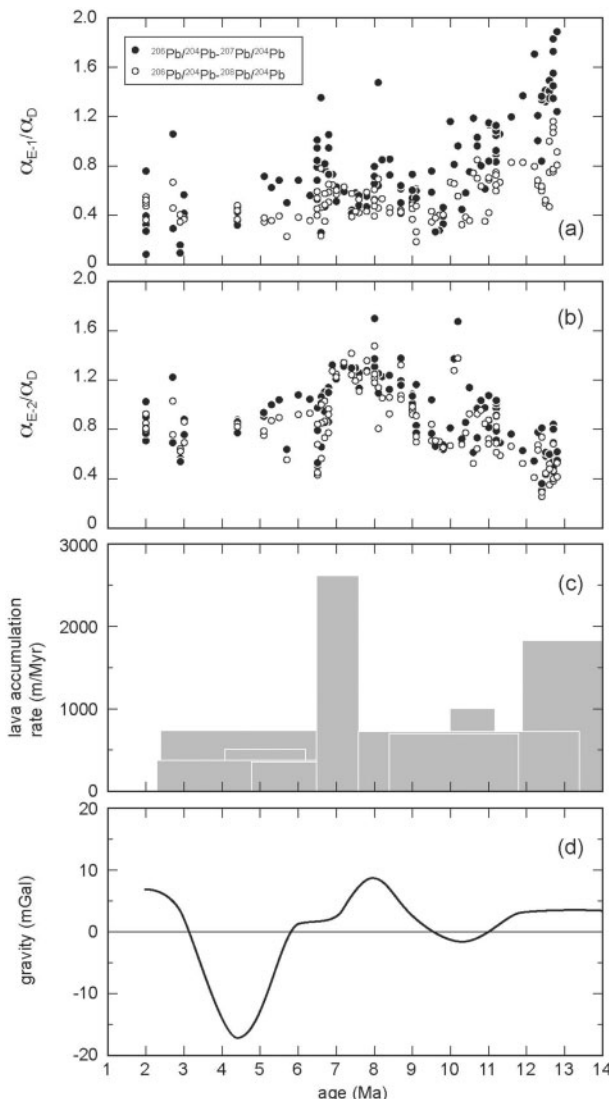


Fig. 13. (a and b) The elemental Pb fractions from the E-1 and E-2 end-member components relative to the proportion from the D end-member component; (c) rate of lava accumulation for paleomagnetic sections in eastern and western Iceland (McDougall *et al.*, 1976a, 1976b, 1977, 1984; Watkins & Walker, 1977; Jancin *et al.*, 1985); (d) profiles of gravity anomaly data obtained from the Irminger Basin with a time shift of +0.5 Myr. The gravity anomaly data are the short-wavelength anomalies relating to the thickness of the crust obtained by subtraction of the long-wavelength anomalies relating to dynamic support driven by the heat of the Iceland mantle plume (Jones *et al.*, 2002).

burial of lavas associated with crustal accretion processes alone (Fig. 13).

Rift relocation versus a pulsing mantle plume

A final issue concerns temporal changes in plume–ridge configuration as a cause of secular changes in the surface magmatism. Over the last 20 Myr, the rift axes have jumped eastwards in a series of steps so as to remain

above the center of the Iceland mantle plume (e.g. Sæmundsson, 1974; Hardarson *et al.*, 1997; Garcia *et al.*, 2003). Hardarson *et al.* (1997) suggested that temporal variations in magma productivity may be caused by rift relocation on the basis of an assumption that the mantle plume has been in a steady state in terms of composition and upwelling mass flux. They assumed that rift relocation plays a role in altering the pattern of mantle flow from the plume into the rift as a result of changes in distance between the center of the mantle plume and the spreading axis. As the spreading axis moves away from the mantle plume, magma productivity should decrease gradually. Hardarson *et al.* (1997) attributed the prominent V-shaped ridges in the sea floor south of Iceland to periodic relocations of the rift axis. However, recent numerical experiments have suggested that relocation of the spreading axis would be unlikely to disrupt the upwelling flow of the mantle plume (Ito, 2001; Jones *et al.*, 2002). This is because the base of the rheological plate probably corresponds to the dry solidus (i.e. dehydration boundary), which probably lies at a constant depth of around 100 km and is independent of lithospheric age (Ito, 2001; Jones *et al.*, 2002). Ito and Jones *et al.* proposed that the major cause of the V-shaped ridges is temporal changes in magma productivity caused by fluctuations in temperature (i.e. a pulsing mantle plume). In the following section, we evaluate the relationships between magma productivity and temporal changes in the composition of the magma source, to assess the relative contributions of the source composition to magma productivity.

Correlation between geochemical characteristics and productivity of the Tertiary Icelandic magmatism

Palaeomagnetic studies of the Tertiary lavas from both eastern and western Iceland indicate that there were several distinct periods of high magma productivity, as summarized in Fig. 13. The sea floor south of Iceland, as far away as a few hundred kilometers from Iceland, also records temporal changes in magma productivity during the Tertiary. For example, bathymetric features and gravity anomaly data show fluctuations that could be interpreted in terms of secular changes in magma productivity (e.g. Vogt, 1971; Johansen *et al.*, 1984; Wright & Miller, 1996; Smallwood & White, 1998; Jones *et al.*, 2002). A short-wavelength gravity anomaly profile obtained from the Irminger Basin on the western flank of the Reykjanes Ridge, located over 300 km south of Iceland (Jones *et al.*, 2002), is shown in Fig. 13d, with an applied time shift of +0.5 Ma. This shift results in the gravity peaks corresponding to those in the eruption rate of Icelandic lavas and to peaks in a topographic transect across the Reykjanes Ridge and Faeroe–Iceland–Greenland aseismic ridge (Wright & Miller, 1996). The positive gravity anomalies correlate with the positive depth anomalies, indicating thicker crust produced by increases in the rate of magmatism.

Jones *et al.* (2002) determined a propagation speed of anomalies within the Iceland plume of 200–250 km/Myr using the angle between the V-shaped ridges and the spreading axis, which corresponds to a time shift of +1.2–2.0 Myr. In contrast, Wright & Miller (1996) calculated propagation speeds, based on the lineation of escarpments, ranging from >1000 km/Myr for the youngest escarpment to 160 km/Myr for the oldest escarpment. Using the propagation speed estimated by Wright & Miller (1996), the possible range in acceptable time shifts is calculated to be from +0.3 to 2.5 Myr. A shift of +0.5 Myr falls within this range and so is an acceptable adjustment to align the gravity profile to the record of subaerial Icelandic magmatism. Because the validity of using an elastic correction is not yet clear (Poore *et al.*, 2006), more detailed numerical modeling is beyond the scope of this study. We emphasize, however, that, as shown in Fig. 13, there is a good correlation between the corrected gravity profile and the subaerial lava accumulation rate in Iceland.

To evaluate the relationship between magma productivity and temporal changes in the composition of the magma source, the elemental Pb fractions from the E-1 and E-2 end-member components relative to that of the D end-member component are compared with magma productivity (Fig. 13). During the period around 13 Ma, lavas with larger contributions from the E-1 end-member component erupted in larger volumes and produced relatively thicker sections of lavas. Subsequently, the magma productivity decreased toward 10 Ma as the contribution from the E-1 end-member component declined and the contribution from the E-2 end-member correspondingly increased. At around 10 Ma, the contribution from the D end-member increased (Fig. 12), accompanied by a decrease in magma productivity shown by the negative gravity anomaly. During the subsequent period from 10 to 8–7 Ma, the contribution from the E-2 end-member component increased dramatically. The increase in the E-2 contribution was associated with a significant increase in magma productivity towards 8–7 Ma, demonstrating a link between the source composition and magma productivity. After this period, the contribution from the E-2 end-member component decreased gradually, and the relative proportion of the E-1 and D end-member components increased again, associated with a gentle decrease in magma productivity toward 6.5 Ma. Magma productivity decreased after 6.5–6 Ma, correlated with the eruption of lavas having larger contributions from the D end-member component relative to both the E-1 and E-2 end-member components. The decrease in magma productivity from 6 to 4 Ma is indicated by both the accumulation rate of the subaerial lavas and the gravity anomaly data (Fig. 13). The increasing intensity of the gravity anomaly for crust younger than 4 Ma, however, is not correlated with the subaerial lava accumulation rate in Iceland. The reason for this

discrepancy still remains unconstrained and the relationships between the gravity anomaly data and the estimation of eruption rate for younger lavas (<2 Ma) need to be investigated.

The most likely explanation for the correlation between source composition and productivity for the Tertiary lavas is that the geochemically enriched end-member components (i.e. E-1 and E-2 end-members) are more easily melted than the relatively depleted D end-member component. Thus, melting of source materials rich in the E-1 or E-2 end-members should result in higher melt productivity at a given temperature in the melting region than melting of source material dominated by the D end-member component (e.g. Hirshmann & Stolper, 1996; Yaxley, 2000). This interpretation is consistent with the E-1 and E-2 end-member components having been derived from recycled crustal materials (with low melting temperatures) as deduced from their geochemical and isotopic characteristics. The major and minor element compositions of the lavas also seem to be consistent with this hypothesis: the older lavas (13–11.5 and 9–7 Ma) have lower SiO₂ and CaO, and higher Al₂O₃ and Na₂O contents than the younger lavas (5–2 Ma) (Fig. 2). Hirshmann *et al.* (2003) showed that low SiO₂–CaO and high Al₂O₃–Na₂O melts can be generated experimentally by melting of silicate-deficient pyroxenite, a possible candidate for recycled material in the melting region, at moderately high pressure conditions (~2 GPa), consistent with the setting of Iceland as a juxtaposed hotspot and mid-ocean ridge system. Higher Ni at a given MgO content in the 13–11.5 and 9–7 Ma lavas may also indicate the involvement of recycled crustal lithologies in the source, because these materials (e.g. pyroxenite) are expected to have lower abundances of olivine, which might buffer the Ni content in the melts relative to mantle peridotite (Sobolev *et al.*, 2005).

Implications for the evolution of Icelandic magmatism

Based on the above discussion, temporal variations in composition and the productivity of the Tertiary Icelandic magmatism can be explained by periodic changes in source composition. This may imply periodic transport of recycled materials from deep mantle regions to the shallow melting regime of the upper mantle. Temporal fluctuations in gravity anomaly data for the Irminger Basin appear to be cyclical on time scales of ~5 Myr and can be traced to ~35 Ma (Jones *et al.*, 2002). Indirect effects of such fluctuations in the magmatism can also be detected in other ways. Magmatic underplating related to the activity of the mantle plume rapidly drove regional surface uplift and denudation, resulting in the periodic development of fan deposits along the continental margins surrounding the North Atlantic during the Palaeogene (White & Lovell, 1997). Temporal variations in the flux of Northern Component Water (NCW) were affected by the dynamic support

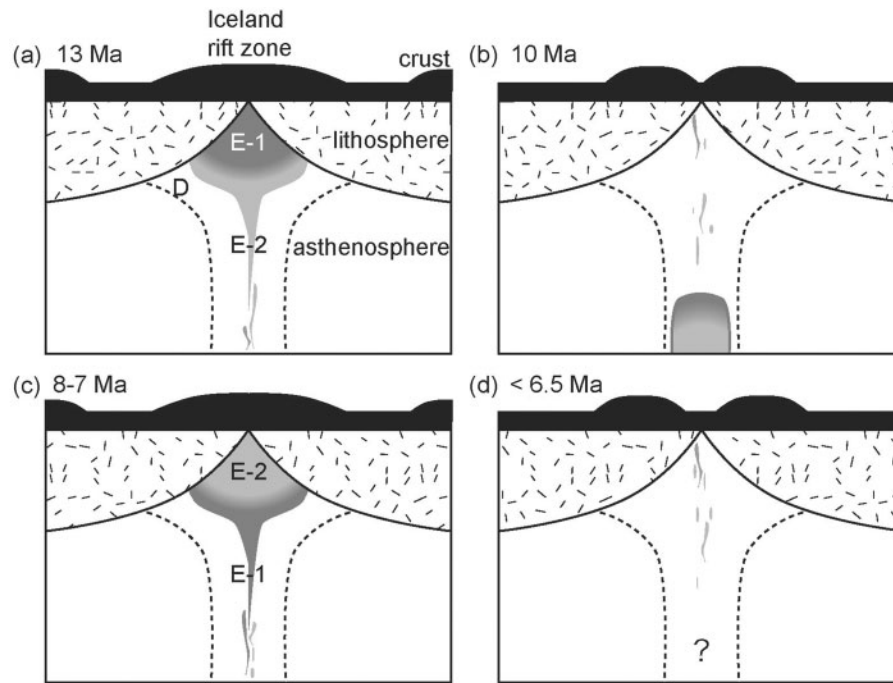


Fig. 14. Schematic diagrams showing the evolution of Icelandic magmatism from 13 to 2 Ma. (a) At c. 13 Ma, a mantle blob dominated by material with the E-1 geochemical signature arrived in the melting region, enhancing magma productivity. The tail of this blob may contain material with E-2 affinity, and thus the magmatism gradually changed from E-1- to E-2-influenced towards >10 Ma. (b) At c. 10 Ma, the mantle blob was partly consumed and the residue was incorporated into the lithosphere. The contribution from the D end-member component correspondingly increased, resulting in eruption of more geochemically depleted magmas and a decline in magma productivity. (c) At 8–7 Ma, a second mantle blob, dominated by the E-2 end-member component, ascended and began to melt, enhancing magma productivity. (d) After 6.5 Ma, the E-2 material rich domain was removed from the stem of mantle plume by extension, and the ensuing magmatism was less voluminous and more geochemically depleted.

that resulted from secular changes in the mantle plume activity during the Neogene: times of high mantle plume activity caused NCW production to cease (Wright & Miller, 1996; Poore *et al.*, 2006). Additionally, seamount basalts from the Atlantic coast of Scotland also record periodic magmatism on time scales of 5–10 Myr (O'Connor *et al.*, 2000). These studies seemingly demonstrate multiple episodes of Icelandic plume magmatism from c. 60 Ma to the present. The similarities between the Tertiary magmatism in the Faeroe Islands (60–50 Ma) and Iceland, in terms of secular variations in production rates and the $(\text{La}/\text{Sm})_n$ ratios of the lavas, also support a model of volumetrically and geochemically periodic magmatism (Noe-Nygaard & Rasmussen, 1968; Schilling & Noe-Nygaard, 1974; Schilling *et al.*, 1982). The blob model [i.e. a pulsing mantle plume, originally proposed by Schilling & Noe-Nygaard (1974)] seems to be an attractive model to account for these observations and for the geochemical data obtained in this study. To explain the observed secular variations in Icelandic magmatism, here we provide a conceptual model for the evolution of the Iceland mantle plume (Fig. 14), based on temporal variations in the geochemistry and productivity of the Tertiary lavas (Figs 12 and 13).

At >13 Ma, a blob dominated by the E-1 end-member component migrated upwards and encountered the melting region, resulting in enhanced magma productivity. A smaller amount of material with the E-2 end-member signature surrounded the tail of this blob. Therefore, from 13 Ma to >10 Ma, the magmatism changed temporally from being E-1 influenced to being E-2 influenced (Figs 12 and 13). Later, at around 10 Ma, this blob had been partly consumed by melting, and the residue became incorporated into the lithosphere. Therefore, the proportion of the D end-member-derived flux increased at c. 10 Ma, and magma productivity correspondingly decreased. During the subsequent period, the next blob ascended into the melting region, resulting in enhanced magma productivity to 8–7 Ma. This blob was mainly composed of the E-2 end-member component, possibly surrounded by the E-1 end-member component. The final stage of melting of this blob at c. 6.5 Ma would thus account for the slightly higher contribution from the E-1 end-member component. Later, this blob also became exhausted, and the contribution from the D end-member component again increased, associated with a decline in magma productivity.

Alternating pulses of blobs relatively rich in the E-1 and E-2 end-member components may have contributed to the

temporal fluctuations in productivity and composition of the Tertiary Icelandic magmatism. An important aspect of our study is that it demonstrates the possibility that discrete mantle blobs containing recycled crustal materials played a major role in controlling the periodic increases in the rate of Icelandic magmatism. Recent numerical modeling (Lin & van Keken, 2005, 2006a, 2006b) demonstrates that the entrainment of dense recycled materials in the source region of a mantle plume can lead to multiple pulses of plume activity, a conclusion seemingly consistent with our model based largely on geochemical data.

CONCLUSIONS

The data presented in this study provide an 11 Myr record of temporal geochemical variations in Icelandic magmatism from 13 to 2 Ma, and yield constraints on the characteristics of the mantle end-member components involved in this magmatism. Temporal variations in the lava geochemistry can be explained by changes in the relative contributions from three mantle end-member components (E-1, E-2 and D), each with distinct geochemical characteristics. Larger contributions from the E-1 end-member component dominate the 13–12 Ma lavas, producing $\Delta 7/4$, $\Delta 8/4$ and $\Delta \epsilon_{\text{Hf}}$ values higher than in lavas from the other periods. The characteristics of another enriched end-member component, E-2, are observed in the 8–7 Ma lavas, and these lavas have the most radiogenic Pb isotope compositions among the eastern Iceland Tertiary lavas. The origin of these two end-member components can be related to recycling of crustal materials. The lavas erupted at c. 10 and 6.5–2 Ma are geochemically less enriched, relative to those from the other periods, and are attributed to melts with a greater contribution from the D end-member component, interpreted to be peridotitic material. The temporal geochemical variations in the Tertiary lavas are well correlated with magma productivity: higher magma productivity is associated with the eruption of geochemically more enriched lavas, whereas lower magma productivity is coincident with the emplacement of less enriched lavas. Correspondence between productivity and the compositions of the Tertiary Icelandic lavas could be due to the periodic entrainment of recycled crustal lithologies into the Iceland plume at its source.

ACKNOWLEDGEMENTS

We are grateful to Y.-H. Lu and all members of the Pheasant Memorial Laboratory for their technical support, constructive discussion and encouragement. We would like to thank T. Yokoyama, K. Kuritani and E. Rose for discussion and help in the sampling, and J. Ó. Fridsteinsson and Á. Höskuldsson for their guidance during the field work in Iceland. We thank I. H. Campbell, K. Grönvold, G. E. Bebout, S.M. Jones, J. MacLennan,

B. N. Nath, B. Paul, R. Tanaka and A. Ishikawa for discussion and improving the manuscript. Thomas Kokfelt, David Peate and one anonymous reviewer are thanked for their helpful reviews, and Colin Devey for his editorial handling. This study was supported by the program ‘Centers of Excellence for 21st century in Japan’ (E.N.), and grants-in-aid for scientific research from MEXT to E.N., A.M., and K.K.

REFERENCES

- Anders, E. & Grevesse, N. (1989). Abundances of the elements: Meteoritic and solar. *Geochimica et Cosmochimica Acta* **53**, 197–214.
- Ayers, J. (1998). Trace element modeling of aqueous fluid–peridotite interaction in the mantle wedge of subduction zones. *Contributions to Mineralogy and Petrology* **132**, 390–404.
- Baker, J., Peate, D., Waught, T. & Meyzen, C. (2004). Pb isotopic analysis of standards and samples using a ^{207}Pb – ^{204}Pb double spike and thallium to correct for mass bias with a double-focusing MC-ICP-MS. *Chemical Geology* **211**, 275–303.
- Baker, J., Peate, D. W., Waught, T. E. & Thirlwall, M. F. (2005). Reply to the: Comment on ‘Pb isotope analysis of standards and samples using a ^{207}Pb – ^{204}Pb double spike and thallium to correct for mass bias with a double focusing MC-ICP-MS’ by Baker *et al.* *Chemical Geology* **217**, 175–179.
- Barker, A., Baker, J. A. & Peate, D. W. (2006). Interaction of the rifting East Greenland margin with a zoned ancestral Iceland plume. *Geology* **34**, 481–484, doi:10.1130/G22366.1.
- Blichert-Toft, J., Frey, F. A. & Albarède, F. (1999). Hf isotope evidence for pelagic sediments in the source of Hawaiian basalts. *Science* **285**, 879–882.
- Blichert-Toft, J., Agranier, A., Andres, M., Kingsley, R., Schilling, J.-G. & Albarède, F. (2005). Geochemical segmentation of the Mid-Atlantic Ridge north of Iceland and ridge–hot spot interaction in the North Atlantic. *Geochemistry, Geophysics, Geosystems* **6**, Q01E19, doi:10.1029/2004GC000788.
- Breddam, K. (2002). Kistfell: Primitive melt from the Iceland mantle plume. *Journal of Petrology* **43**, 345–373.
- Carmichael, I. S. E. (1964). The petrology of Thingmuli, a Tertiary volcano in eastern Iceland. *Journal of Petrology* **5**, 435–460.
- Chauvel, C. & Hémond, C. (2000). Melting of a complete section of recycled oceanic crust: Trace element and Pb isotopic evidence from Iceland. *Geochemistry, Geophysics, Geosystems* **1**, 1999GC000002.
- Dagley, P., Wilson, R. L., Ade-Hall, J. M., Walker, G. P. L., Haggerty, S. E., Sigurgeirsson, T., Watkins, N. D., Smith, P. J., Edwards, J. & Grasty, R. L. (1967). Geomagnetic polarity zones for Icelandic lavas. *Nature* **216**, 25–29.
- Debaille, V., Blichert-Toft, J., Agranier, A., Doucelance, R., Schiano, P. & Albarède, F. (2006). Geochemical component relationships in MORB from the Mid-Atlantic Ridge, 22–35°N. *Earth and Planetary Science Letters* **241**, 844–862.
- Eisele, J., Sharma, M., Galer, S. J. G., Blichert-Toft, J., Devey, C. W. & Hofmann, A. W. (2002). The role of sediment recycling in EM-1 inferred from Os, Pb, Hf, Nd, Sr isotope and trace element systematics of the Pitcairn hotspot. *Earth and Planetary Science Letters* **196**, 197–212.
- Elliott, T. R., Hawkesworth, C. J. & Grönvold, K. (1991). Dynamic melting of the Iceland plume. *Nature* **351**, 201–206.
- Fitton, J. G., Saunders, A. D., Norry, M. J., Hardarson, B. S. & Taylor, R. N. (1997). Thermal and chemical structure of the Iceland plume. *Earth and Planetary Science Letters* **153**, 197–208.

- Fitton, J. G., Saunders, A. D., Kempton, P. D. & Hardarson, B. S. (2003). Does depleted mantle form an intrinsic part of the Iceland plume? *Geochemistry, Geophysics, Geosystems* **4**, doi:10.1029/2002GC000424.
- Garcia, S., Arnaud, N. O., Angelier, J., Bergerat, F. & Homberg, C. (2003). Rift jump process in Northern Iceland since 10 Ma from $^{40}\text{Ar}/^{39}\text{Ar}$ geochronology. *Earth and Planetary Science Letters* **214**, 529–544.
- Hanan, B. B. & Graham, D. W. (1996). Lead and helium isotope evidence from oceanic basalts for a common deep source of mantle plumes. *Science* **272**, 991–995.
- Hanan, B. B. & Schilling, J.-G. (1997). The dynamic evolution of the Iceland mantle plume: the lead isotope perspective. *Earth and Planetary Science Letters* **151**, 43–60.
- Hanan, B. B., Blöcher-Toft, J., Kingsley, R. & Schilling, J.-G. (2000). Depleted Iceland mantle plume geochemical signature: Artifact of multicomponent mixing? *Geochemistry, Geophysics, Geosystems* **1**, 1999GC000009.
- Hanan, B. B., Blöcher-Toft, J., Pyle, D. G. & Christie, D. M. (2004). Contrasting origins of the upper mantle revealed by hafnium and lead isotopes from the Southeast Indian Ridge. *Nature* **432**, 91–94.
- Hardarson, B. S. & Fitton, J. G. (1997). Mechanisms of crustal accretion in Iceland. *Geology* **25**, 1043–1046.
- Hardarson, B. S., Fitton, J. G., Ellam, R. M. & Pringle, M. S. (1997). Rift relocation—a geochemical and geochronological investigation of a palaeo-rift in northwest Iceland. *Earth and Planetary Science Letters* **153**, 181–196.
- Hards, V. L., Kempton, P. D. & Thompson, R. N. (1995). The heterogeneous Iceland plume: new insights from the alkaline basalts of the Snæfells volcanic centre. *Journal of the Geological Society, London* **152**, 1003–1009.
- Hards, V. L., Kempton, P. D., Thompson, R. N. & Greenwood, P. B. (2000). The magmatic evolution of the Snæfells volcanic centre; an example of volcanism during incipient rifting in Iceland. *Journal of Volcanology and Geothermal Research* **99**, 97–121.
- Hart, S. R. (1984). A large-scale isotope anomaly in the Southern Hemisphere mantle. *Nature* **309**, 753–757.
- Hemond, C., Arndt, N. T., Lichtenstein, U., Hofmann, A. W., Oskarsson, N. & Steinþorsson, S. (1993). The heterogeneous Iceland plume: Nd–Sr–O isotopes and trace element constraints. *Journal of Geophysical Research* **98**, 15833–15850.
- Hirshmann, M. M. & Stolper, E. M. (1996). A possible role for garnet pyroxenite in the origin of the ‘garnet signature’ in MORB. *Contributions to Mineralogy and Petrology* **124**, 185–208.
- Hirshmann, M. M., Kogiso, T., Baker, M. B. & Stolper, E. M. (2003). Alkalic magmas generated by partial melting of garnet pyroxenite. *Geology* **31**, 481–483.
- Irvine, T. N. & Baragar, W. R. A. (1971). A guide to the chemical classification of the common volcanic rocks. *Canadian Journal of Earth Sciences* **8**, 523–548.
- Ito, G. (2001). Reykjanes ‘V’-shaped ridges originating from a pulsing and dehydrating mantle plume. *Nature* **411**, 681–684.
- Jancin, M., Young, K. D., Voight, B., Aronson, J. L. & Sæmundsson, K. (1985). Stratigraphy and K/Ar ages across the west flank of the northeast Iceland axial rift zone, in relation to the 7 Ma volcano-tectonic reorganization of Iceland. *Journal of Geophysical Research* **90**, 9961–9985.
- Johansen, B., Vogt, P. R. & Eldholm, O. (1984). Reykjanes Ridge: further analysis of crustal subsidence and time transgressive basement topography. *Earth and Planetary Science Letters* **68**, 249–258.
- Jones, S. M., White, N. & MacLennan, J. (2002). V-shaped ridges around Iceland: Implications for spatial and temporal patterns of mantle convection. *Geochemistry, Geophysics, Geosystems* **3**, doi:10.1029/2002GC000361.
- Kempton, P. D., Fitton, J. G., Saunders, A. D., Nowell, G. M., Taylor, R. N., Hardarson, B. S. & Pearson, G. (2000). The Iceland plume in space and time: a Sr–Nd–Pb–Hf study of the North Atlantic rifted margin. *Earth and Planetary Science Letters* **177**, 255–271.
- Kokfelt, T. F., Hoernle, K., Hauff, F., Fiebig, J., Werner, R. & Garbe-Schönberg, D. (2006). Combined trace element and Pb–Nd–Sr–O isotope evidence for recycled oceanic crust (upper and lower) in the Iceland mantle plume. *Journal of Petrology* **47**, 1705–1749.
- Kuritani, T. & Nakamura, E. (2003). Highly precise and accurate isotopic analysis of small amounts of Pb using ^{205}Pb – ^{204}Pb and ^{207}Pb – ^{204}Pb , two double spikes. *Journal of Analytical and Atomic Spectrometry* **18**, 1464–1470.
- Lin, S.-C. & van Keken, P. E. (2005). Multiple volcanic episodes of flood basalts caused by thermochemical mantle plumes. *Nature* **436**, 250–252.
- Lin, S.-C. & van Keken, P. E. (2006a). Dynamics of thermochemical plumes: I. Plume formation and entrainment of a dense layer. *Geochemistry, Geophysics, Geosystems* **7**, Q02006, doi:10.1029/2005GC001071.
- Lin, S.-C. & van Keken, P. E. (2006b). Dynamics of thermochemical plumes: 2. Complexity of plume structures and its implications for mapping mantle plumes. *Geochemistry, Geophysics, Geosystems* **7**, Q03003, doi:10.1029/2005GC001072.
- Lu, Y., Makishima, A. & Nakamura, E. (2007a). Coprecipitation of Ti, Mo, Sn and Sb with fluorides and application to determination of B, Ti, Zr, Nb, Mo, Sn, Sb, Hf and Ta by ICP-MS. *Chemical Geology* **236**, 13–26.
- Lu, Y., Makishima, A. & Nakamura, E. (2007b). Purification of Hf in silicate materials using extraction chromatographic resin, and its application to precise determination of $^{176}\text{Hf}/^{177}\text{Hf}$ by MC-ICP-MS with ^{179}Hf spike. *Journal of Analytical and Atomic Spectrometry* **22**, 69–76, doi:10.1039/b610197f.
- Makishima, A. & Nakamura, E. (1997). Suppression of matrix effects in ICP-MS by high power operation of ICP: Application to precise determination of Rb, Sr, Y, Cs, Ba, REE, Pb, Th and U at ng g⁻¹ levels in milligram silicate samples. *Geostandards Newsletter* **21**, 307–319.
- Makishima, A. & Nakamura, E. (2006). Determination of major, minor and trace elements in silicate samples by ICP-QMS and ICP-SFMS applying isotope dilution-internal standardisation (ID-IS) and multi-stage internal standardisation. *Geostandards and Geoanalytical Research* **30**, 245–271.
- Makishima, A., Nakamura, E. & Nakano, T. (1997). Determination of boron in silicate samples by direct aspiration of sample HF solutions into ICPMS. *Analytical Chemistry* **69**, 3754–3759.
- Makishima, A., Nakamura, E. & Nakano, T. (1999). Determination of zirconium, niobium, hafnium and tantalum at ng g⁻¹ levels in geological materials by direct nebulisation of sample HF solution into FI-ICP-MS. *Geostandards Newsletter* **23**, 7–20.
- McDonough, W. F. & Sun, S.-s. (1995). The composition of the Earth. *Chemical Geology* **120**, 223–253.
- McDougall, I., Watkins, N. D. & Kristjansson, L. (1976a). Geochronology and paleomagnetism of a Miocene–Pliocene lava sequence at Bessastadara, eastern Iceland. *American Journal of Science* **276**, 1078–1095.
- McDougall, I., Watkins, N. D., Walker, G. P. L. & Kristjansson, L. (1976b). Potassium–argon and paleomagnetic analysis of Icelandic lava flows: Limits on the age of anomaly 5. *Journal of Geophysical Research* **81**, 1505–1512.

- McDougall, I., Sæmundsson, K., Johannesson, H., Watkins, N. D. & Kristjansson, L. (1977). Extension of the geomagnetic polarity time scale to 6.5 m.y.: K-Ar dating, geological and paleomagnetic study of a 3,500-m lava succession in western Iceland. *Geological Society of America Bulletin* **88**, 1–15.
- McDougall, I., Kristjansson, L. & Sæmundsson, K. (1984). Magnetostratigraphy and geochronology of northwest Iceland. *Journal of Geophysical Research* **89**, 7029–7060.
- Mertz, D. F. & Haase, K. M. (1997). The radiogenic isotope composition of the high-latitude North Atlantic mantle. *Geology* **25**, 411–414.
- Mertz, D. F., Devey, C. W., Todt, W., Stoffers, P. & Hofmann, A. W. (1991). Sr-Nd-Pb isotope evidence against plume–asthenosphere mixing north of Iceland. *Earth and Planetary Science Letters* **107**, 243–255.
- Morgan, W. J. (1971). Convection plumes in the lower mantle. *Nature* **230**, 42–43.
- Moriguti, T., Makishima, A. & Nakamura, E. (2004). Determination of lithium contents in silicates by isotope dilution ICP-MS and its evaluation by isotope dilution thermal ionisation mass spectrometry. *Geostandards and Geoanalytical Research* **28**, 371–382.
- Mussett, A. E., Ross, J. G. & Gibson, I. L. (1980). $^{40}\text{Ar}/^{39}\text{Ar}$ dates of eastern Iceland lavas. *Geophysical Journal of the Royal Astronomical Society* **60**, 37–52.
- Nakamura, E., Makishima, A., Moriguti, T., Kobayashi, K., Sakaguchi, C., Yokoyama, T., Tanaka, R., Kuritani, T. & Takei, H. (2003). Comprehensive geochemical analyses of small amounts (<100 mg) of extraterrestrial samples for the analytical competition related to the sample return mission MUSES-C. *Institute of Space and Astronautical Science Report SP* **16**, 49–101.
- Noe-Nygaard, A. & Rasmussen, J. (1968). Petrology of a 3,000 metre sequence of basaltic lavas in the Faeroe Islands. *Lithos* **1**, 286–304.
- O'Connor, J. M., Stoffers, P., Wijbrans, J. R., Shannon, P. M. & Morrissey, T. (2000). Evidence from episodic seamount volcanism for pulsing of the Iceland mantle plume in the past 70 Myr. *Nature* **408**, 954–958.
- O'Nions, R. K. & Pankhurst, R. J. (1973). Secular variation in the Sr-isotope composition of Icelandic volcanic rock. *Earth and Planetary Science Letters* **21**, 13–21.
- Óskarsson, N., Steinþorsson, S. & Sigvaldason, G. E. (1985). Iceland geochemical anomaly: origin, volcanotectonics, chemical fractionation and isotope evolution of the crust. *Journal of Geophysical Research* **90**, 10011–10025.
- Pálmasón, G. & Sæmundsson, K. (1974). Iceland in relation to the Mid-Atlantic Ridge. *Annual Review of Earth and Planetary Sciences* **2**, 25–50.
- Patchett, P. J., White, W. M., Feldmann, H., Kielinczuk, S. & Hofmann, A. W. (1984). Hafnium/rare earth element fractionation in the sedimentary system and crustal recycling into the Earth's mantle. *Earth and Planetary Science Letters* **69**, 365–378.
- Plank, T. & Langmuir, C. H. (1998). The chemical composition of subducting sediment and its consequences for the crust and mantle. *Chemical Geology* **145**, 325–394.
- Poore, H. R., Samworth, R., White, N. J., Jones, S. M. & McCave, I. N. (2006). Neogene overflow of Northern Component Water at the Greenland–Scotland Ridge. *Geochemistry, Geophysics, Geosystems* **7**, Q06010, doi:10.1029/2005GC001085.
- Prestvik, T., Goldberg, S., Karlsson, H. & Grönvold, K. (2001). Anomalous strontium and lead isotope signatures in the off-rift Öraefajökull central volcano in south-east Iceland. Evidence for enriched endmember(s) of the Iceland mantle plume? *Earth and Planetary Science Letters* **190**, 211–220.
- Ross, J. G. & Mussett, A. E. (1976). $^{40}\text{Ar}/^{39}\text{Ar}$ dates for spreading rates in eastern Iceland. *Nature* **259**, 36–38.
- Rudnick, R. L. & Fountain, D. M. (1995). Nature and composition of the continental crust: a lower crustal perspective. *Reviews of Geophysics* **33**, 267–309.
- Rudnick, R. L. & Goldstein, S. L. (1990). The Pb isotopic compositions of lower crustal xenoliths and the evolution of lower crustal Pb. *Earth and Planetary Science Letters* **98**, 192–207.
- Saunders, A. D., Fitton, J. G., Kerr, A. C., Norry, M. J. & Kent, R. W. (1997). The North Atlantic Igneous Province. In: Mahoney, J. J. & Coffin, M. F. (eds) *Large Igneous Provinces: Continental, Oceanic, and Planetary Flood Volcanism*. American Geophysical Union, *Geophysical Monograph* **100**, 45–93.
- Sæmundsson, K. (1974). Evolution of the axial rifting zone in northern Iceland and the Tjörnes fracture zone. *Geological Society of America Bulletin* **85**, 495–504.
- Schilling, J.-G. (1973). Iceland mantle plume: geochemical study of Reykjanes Ridge. *Nature* **242**, 565–571.
- Schilling, J.-G. & Noe-Nygaard, A. (1974). Faeroe–Iceland plume: rare-earth evidence. *Earth and Planetary Science Letters* **24**, 1–14.
- Schilling, J.-G., Meyer, P. S. & Kingsley, R. H. (1982). Evolution of the Iceland hotspot. *Nature* **296**, 313–320.
- Schilling, J.-G., Kingsley, R., Fontignie, D., Poreda, R. & Xue, S. (1999). Dispersion of the Jan Mayen and Iceland mantle plumes in the Arctic: A He–Pb–Nd–Sr isotope tracer study of basalts from the Kolbeinsey, Mohns, and Knipovich Ridges. *Journal of Geophysical Research* **104**, 10543–10569.
- Schilling, J.-G., Fontignie, D., Blachert-Toft, J., Kingsley, R. & Tomza, U. (2003). Pb–Hf–Nd–Sr isotope variations along the Galápagos Spreading Center (101° – 83° W): Constraints on the dispersal of the Galápagos mantle plume. *Geochemistry, Geophysics, Geosystems* **4**, doi:10.1029/2002GC000495.
- Schmitz, M. D., Vervoort, J. D., Bowring, S. A. & Patchett, P. J. (2004). Decoupling of the Lu–Hf and Sm–Nd isotope systems during the evolution of granulitic lower crust beneath southern Africa. *Geology* **32**, 405–408.
- Skovgaard, A. C., Storey, M., Baker, J., Blusztajn, J. & Hart, S. (2000). Osmium–oxygen isotopic evidence for a recycled and strongly depleted component in the Iceland mantle plume. *Earth and Planetary Science Letters* **194**, 259–275.
- Smallwood, J. R. & White, R. S. (1998). Crustal accretion at the Reykjanes Ridge, 61° – 62° N. *Journal of Geophysical Research* **103**, 5185–5201.
- Sobolev, A. V., Hofmann, A. W., Sobolev, S. V. & Nikogosian, I. K. (2005). An olivine-free mantle source of Hawaiian shield basalts. *Nature* **434**, 590–597.
- Stalder, R., Foley, S. F., Brey, G. P. & Horn, I. (1998). Mineral–aqueous fluid partitioning of trace elements at 900 – 1200°C and 3.0 – 5.7 GPa: New experimental data for garnet, clinopyroxene, and rutile, and implications for mantle metasomatism. *Geochimica et Cosmochimica Acta* **62**, 1781–1801.
- Stecher, O., Carlson, R. W. & Gunnarsson, B. (1999). Torfajökull: a radiogenic end-member of the Iceland Pb-isotope array. *Earth and Planetary Science Letters* **165**, 117–127.
- Storey, M., Duncan, R. A. & Swisher, C. C., III (2007a). Paleocene–Eocene Thermal Maximum and the opening of the Northeast Atlantic. *Science* **316**, 587–589.
- Storey, M., Duncan, R. A. & Tegner, C. (2007b). Timing and duration of volcanism in the North Atlantic Igneous Province: Implications for geodynamics and links to the Iceland hotspot. *Chemical Geology* **241**, 264–281.
- Stracke, A., Bizimis, M. & Salters, V. J. M. (2003a). Recycling oceanic crust: Quantitative constraints. *Geochemistry, Geophysics, Geosystems* **4**, doi:10.1029/2001GC000223.

- Stracke, A., Zindler, A., Salters, V. J. M., McKenzie, D., Blichert-Toft, J., Albarède, F. & Grönvold, K. (2003b). Theistareykir revisited. *Geochemistry, Geophysics, Geosystems* **4**, doi:10.1029/2001GC000201.
- Stracke, A., Hofmann, A. W. & Hart, S. R. (2005). FOZO, HIMU, and the rest of the mantle zoo. *Geochemistry, Geophysics, Geosystems* **6**, Q05007, doi:10.1029/2004GC000824.
- Sun, S.-S. & Jahn, B.-m. (1975). Lead and strontium isotopes in post-glacial basalts from Iceland. *Nature* **255**, 527–530.
- Sun, S.-S., Tatsumoto, M. & Schilling, J.-G. (1975). Mantle plume mixing along the Reykjanes axis: Lead isotope evidence. *Science* **190**, 143–147.
- Takei, H. (2002). Development of precise analytical techniques for major and trace element concentrations in rock samples and their applications to the Hishikari Gold Mine, southern Kyushu, Japan. PhD thesis, Okayama University, 164 pp.
- Taylor, R. N., Thirlwall, M. F., Murton, B. J., Hilton, D. R. & Gee, M. A. M. (1997). Isotopic constraints on the influence of the Iceland plume. *Earth and Planetary Science Letters* **148**, E1–E8.
- Thirlwall, M. F., Gee, M. A. M., Taylor, R. N. & Murton, B. J. (2004). Mantle components in Iceland and adjacent ridges investigated using double-spike Pb isotope ratios. *Geochimica et Cosmochimica Acta* **68**, 361–386.
- Vervoort, J. D., Patchett, P. J., Blichert-Toft, J. & Albarède, F. (1999). Relationships between Lu–Hf and Sm–Nd isotopic systems in the global sedimentary system. *Earth and Planetary Science Letters* **168**, 79–99.
- Vogt, P. R. (1971). Asthenosphere motion recorded by the ocean floor south of Iceland. *Earth and Planetary Science Letters* **13**, 153–160.
- Walker, G. P. L. (1959). Geology of the Reydarfjördur area, eastern Iceland. *Quarterly Journal of Geological Society of London* **114**, 367–393.
- Walker, G. P. L. (1964). Geological investigations in eastern Iceland. *Bulletin of Volcanology* **27**, 351–363.
- Watkins, N. D. & Walker, G. P. L. (1977). Magnetostratigraphy of eastern Iceland. *American Journal of Science* **277**, 513–584.
- Welke, H., Moorbat, S. & Cumming, G. L. (1968). Lead isotope studies on igneous rocks from Iceland. *Earth and Planetary Science Letters* **4**, 221–231.
- White, N. & Lovell, B. (1997). Measuring the pulse of a plume with sedimentary record. *Nature* **387**, 888–891.
- Wood, D. A. (1976). Spatial and temporal variation in the trace element geochemistry of the eastern Iceland flood basalt succession. *Journal of Geophysical Research* **81**, 4353–4360.
- Wood, D. A. (1978). Major and trace element variations in the Tertiary lavas of eastern Iceland and their significance with respect to the Iceland geochemical anomaly. *Journal of Petrology* **19**, 393–436.
- Wood, D. A., Gibson, I. L. & Thompson, R. N. (1976). Elemental mobility during zeolite facies metamorphism of the Tertiary basalts of eastern Iceland. *Contributions to Mineralogy and Petrology* **55**, 241–254.
- Wright, J. D. & Miller, K. G. (1996). Control of North Atlantic Deep Water circulation by the Greenland–Scotland Ridge. *Paleoceanography* **11**, 157–170.
- Yaxley, G. M. (2000). Experimental study of the phase and melting relations of homogeneous basalt + peridotite mixtures and implications for the petrogenesis of flood basalts. *Contributions to Mineralogy and Petrology* **139**, 326–338.
- Yoder, H. S. & Tilley, C. E. (1962). Origin of basalt magmas: an experimental study of natural and synthetic rock systems. *Journal of Petrology* **3**, 342–532.
- Yokoyama, T. & Nakamura, E. (2002). Precise determination of ferrous iron in silicate rocks. *Geochimica et Cosmochimica Acta* **66**, 1085–1093.
- Yokoyama, T., Makishima, A. & Nakamura, E. (1999). Evaluation of the coprecipitation of incompatible trace elements with fluoride during silicate rock dissolution by acid digestion. *Chemical Geology* **157**, 175–187.
- Yoshikawa, M. & Nakamura, E. (1993). Precise isotope determination of trace amounts of Sr in magnesium-rich samples. *Journal of Mineralogist, Petrologist and Economic Geologist* **88**, 548–561.
- Zindler, A. & Hart, S. (1986). Chemical geodynamics. *Annual Review of Earth and Planetary Sciences* **14**, 493–571.
- Zindler, A., Hart, S. R., Frey, F. A. & Jakobsson, S. P. (1979). Nd and Sr isotope ratios and rare earth element abundances in Reykjanes Peninsula basalts: Evidence for mantle heterogeneity beneath Iceland. *Earth and Planetary Science Letters* **45**, 249–262.